2.2 Effect of histamine on the type I hypersensitivity reaction

We observed the skin reaction to the mast cell secretagogue, compound 48/80, in both HDC(–/–) and HDC(+/+) mice. Compound 48/80 efficiently releases histamine from mast cells after subcutaneous administration. When HDC(–/–) mice were treated with this compound, no skin extravasation reaction was observed (Fig. 1A). The injection of histamine itself evoked an extravasation reaction in both genotypes (Fig. 1A). We kept the animals on the L+H diet for 7 days to increase the tissue histamine level. The skin of both HDC(+/+) and HDC(–/–) mice lost the response to histamine and compound 48/80 (Fig. 1B), suggesting that desensitization had occurred with the high amount of histamine. The response was restored to the wild-type mice 4 days after changing to the L diet (Fig. 1C), suggesting that reactivation of the histamine receptors had occurred. Interestingly, the extravasation reaction was observed with compound 48/80 in HDC(–/–) mice after the same dietary control (Fig. 1C).

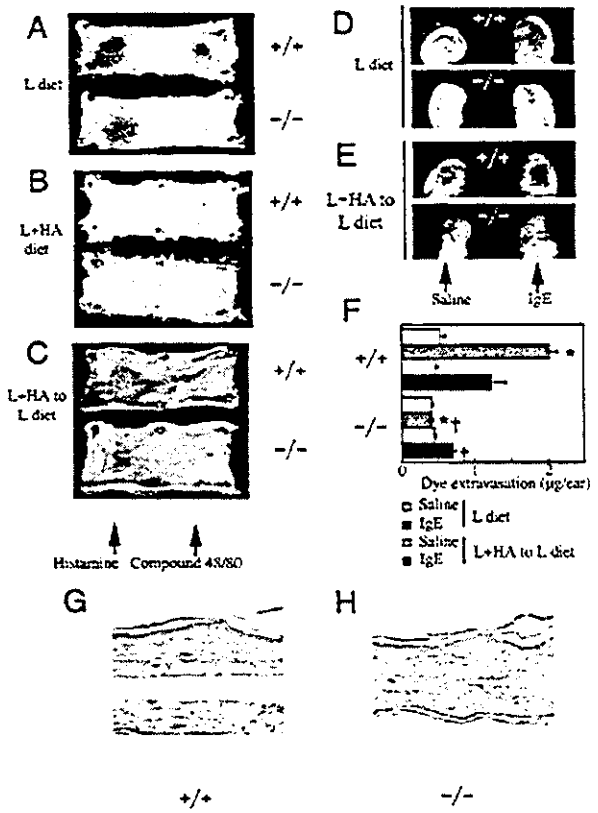

Fig. 1. Histamine dependence of skin allergic extravasation reactions. (A–C) Reaction to histamine and compound 48/80. (A) L diet; (B) L+HA diet; (C) switched from L+HA to L. (D–F) PCA test. (D) L diet; (E) switched from L+HA to L. (F) Quantification of the Evans' blue dye in the PCA reaction. After the extraction, the dye was colorimetrically quantified at 620 nm. The amount of the dye extravasation was represented as mean ± SE. The sample size varied between n=3 and 8. (G, H) H&E staining of the ear of PCA reaction. The section was made at 30 min after PCA reaction in the (G) HDC(+/+) and (H) HDC(–/–) mice. ×200.

The concentration of histamine in the skin of the HDC(–/–) mice kept only on the L diet was 0.26 ±0.06 nmol/g (n=4) (Table 1). The mice switched to the L+HA diet for 7 days showed an increase in histamine to 10.53±0.65 nmol/g in the skin tissue (Table 1). After reverting back to the L diet for 4 days, the level of histamine was reduced to 3.9±0.5 nmol/g skin, which was still significantly higher (p<0.02, n=4) than the initial value. In contrast, the concentration in the plasma was considerably decreased after reverting to the L diet for 4 days (0.16±0.00 nmol/ml plasma, where the initial value was 0.04±0.01 nmol/ml) compared to the mice kept on the L+HA diet for 7 days (11.3±1.25 nmol/ml). This may reflect the absorption of histamine into histamine-releasing cells, which leads to the recovery from desensitisation.

We observed a distinct dye extravasation reaction in the wild-type mice with the passive cutaneous anaphylaxis (PCA) test (Fig. 1D). In contrast, no extravasation was observed in the HDC(–/–) mice (Fig. 1D). The mean amount of local dye extravasation of the wild-type mice

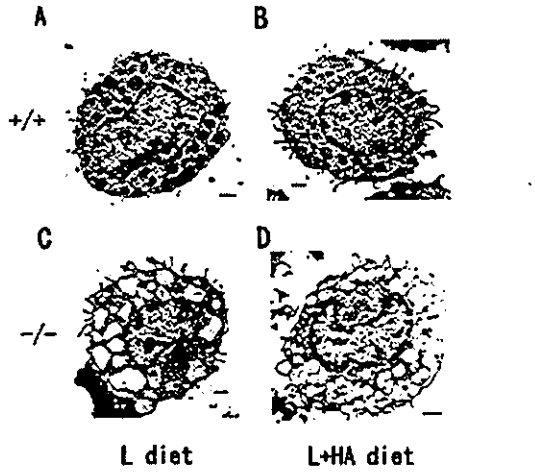

Fig. 2. Transmission electron microscopy of mast cells from the peritoneum of the HDC(+/+) mice (A, B) and HDC(–/–) mice (C, D). The mice were fed under L (A, C) or L+HA (B, D) conditions for 7 days. Peritoneal cells were washed with PBS and fixed in Karnovsky's for embedding in epoxy resin. ×3,000.

was five times higher than that of HDC(–/–) mice in the PCA reaction (compare the bars with *; Fig. 1F). Histological study revealed that these plasma exudates produced inter-tissue edema in HDC(+/+) mice, although it was not observed in HDC(–/–) mice, 30 min after the DNP-HSA challenge (Fig. 1G, H). The plasma extravasation reaction was abolished in the mice on a L+HA diet for 7 days (data not shown), but was again observed even in HDC(–/–) mice after 4 days under the L diet condition (Fig. 1E). The amount of extracted Evans' blue in the PCA reaction was significantly increased after the HDC(–/–) mice were kept on the L+HA diet for 7 days and on the L diet for 4 days compared to those mice kept only on the L diet (compare the bars with †; Fig. 1F). These findings suggest that histamine is one of the primary effectors in the PCA reaction and that there was uptake and storage of exogenous histamine by mast cells of the skin of HDC(–/–) mice.

In electron micrographic study the mast cells from the HDC(–/–) mice showed a reduced granular content (Fig. 2C, D). This reduction was not changed in HDC(–/–) mice by the L+HA diet. Therefore, it is difficult to imagine that other intragranular mediators were replenished under the effect of the dietary supplemented histamine and produced the plasma extravasation reaction in HDC(–/–) mice.

2.3 Effect of histamine on the type IV hypersensitivity reaction

We next used the hapten-specific CH responses as a type of DTH reaction of the skin. In the CH model the ear thickness in HDC(–/–) mice was not significantly different from that in the wild-type mice at any time point as shown in Fig. 3, suggesting that histamine is not strongly involved in the skin swelling in the DTH.

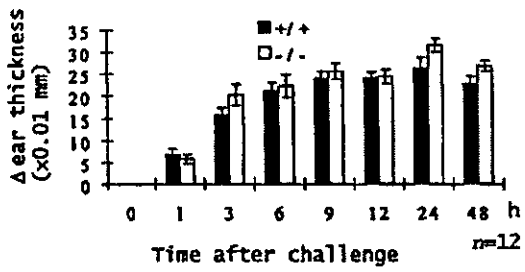

Fig. 3. Time course of TNCB-specific ear swelling response in HDC(+/+) and HDC(–/–) mice. The mice were sensitized in the right ear with TNCB 7 days before the challenge. Ear swelling responses were measured at several time points after challenge. The kinetics of ear-swelling responses (the mean ± SEM) is shown.

2.4 Histamine absorption in bone marrow-derived mast cell *in vitro*

Bone marrow-derived mast cells (BMMC) from each genotype were incubated in the culture medium supplemented with [^{3}H]histamine, and its uptake was measured as the radioactivity count of the cell pellet after washing out the free isotope. BMMC rapidly took up [^{3}H]histamine at 37°C at a rate of approximately 50 fmol/mg protein/min, while they did not take up any tracer at 0°C (Fig. 4A). The uptake of histamine into the mast cells is a temperature-dependent reaction. The uptake rates of histamine in BMMC of HDC(–/–) mice were close to those of HDC(+/+) mice. To examine the specificity of histamine uptake, the cells were first incubated with various concentrations of histamine at 0°C, then at 37°C with 1.5 nM of [^{3}H]histamine for 10 min and the uptake of the [^{3}H]histamine was calculated. Cold histamine inhibited the uptake of [^{3}H]histamine in a dose-related manner and the fashion of this inhibition was quite similar between the two genotypes (Fig. 4B). Scatchard analysis revealed K_i values of 0.72 mM for the wild-type and

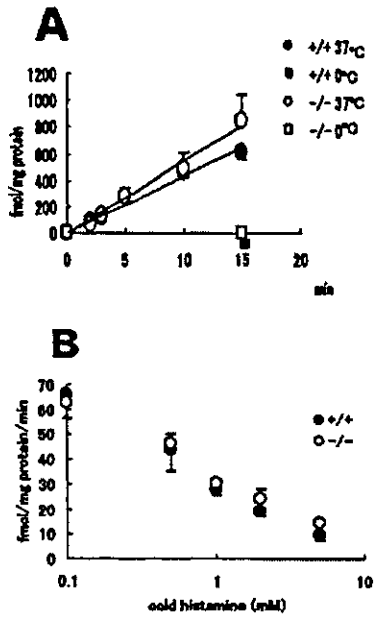

Fig. 4. (A) [^{3}H]Histamine uptake into BMMC from HDC(+/+) and HDC(–/–) mice. The cells were incubated at 4°C or 37°C for various periods with ^{3}H-labeled histamine. Cells were washed, and collected on a glass filter. Absorbed [^{3}H]histamine was calculated after counting the radioactivity on the glass filter. (B) After pretreatment of the cells with various concentrations of cold histamine for 10 min, the cells were incubated with 1.5 nM of [^{3}H]histamine for 10 min. Absorbed [^{3}H]histamine was calculated as described above. The rate of uptake of [^{3}H]histamine into the cells is expressed against the concentration of the cold histamine.

0.60 mM for the knockout mast cells. These data indicated that intrinsic histamine does not grossly influence the kinetics of the histamine uptake by BMMC.

The BMMC continuously took up histamine at a constant pace until 60 min at the two different histamine concentrations (10 μM and 100 μM) (Fig. 5A). We incubated the BMMC of HDC(−/−) mice in various concentrations of histamine-containing medium for 30 min and measured the histamine content in the cells. The speed of histamine absorption of the cells increased dose dependently (Fig. 5B). Transforming these data using the Rosenthal-Scatchard equation suggested the existence of two components in the transporting system; one with low affinity (K_m=1.6 mM) and high capacity (V_{max}=617 pmol/mg protein/min) and the other one with high affinity (K_m=0.09 mM) and low capacity (V_{max}=68 pmo/mg protein/min) (Fig. 5C).

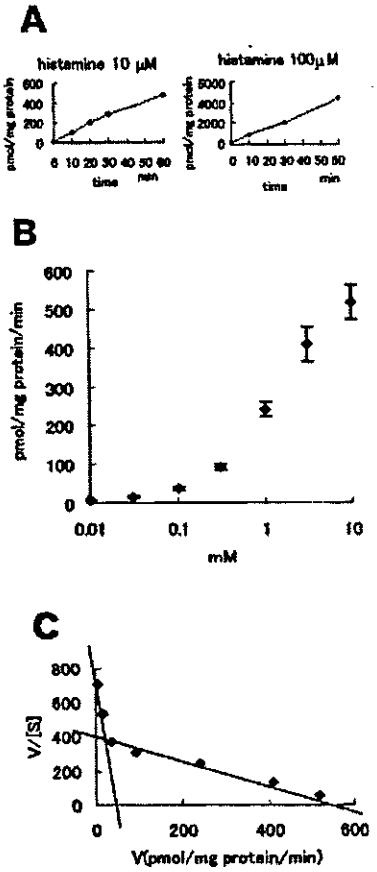

Fig. 5. (A) Cold histamine uptake into the BMMC from the HDC(−/−) mice. Cold histamine was added to the medium (10 μM and 100 μM final concentration) and the uptake measured. Absorbed histamine was plotted against incubation time. (B) The mean rate of uptake for the initial 30-min incubation was calculated and plotted against the concentration of histamine. (C) The figure shown in (B) was transformed as a Rosenthal-Scatchard plot. The distribution of the data shows a concave form and two regression lines can be drawn for this curve.

We used a dopamine transporter inhibitor (GBR-12909) and a noradrenaline transporter inhibitor (maprotiline). These two transporter inhibitors had no inhibitory effect on the uptake of histamine into BMMC (Table 2). On the other hand, tetrabenazine, one of the vesicular monoamine transporter2 (VMAT2) inhibitors, had an inhibitory effect on the uptake of histamine (Table 2). It is known that VMAT2 knockout mice show a significant reduction in the granular contents including serotonin and histamine in BMMC [12]. The IC_{50} of tetrabenazine was about 1.25 μM for histamine uptake, suggesting that VMAT2 is an important vesicular membrane transporter in histamine uptake.

We assessed the histamine uptake in the presence of three kinds of histamine receptor antagonists; D-chlorpheniramine for the H1 receptor, famotidine for the H2 receptor, and thioperamide for the H3 receptor. These three receptor antagonists did not inhibit the uptake of the histamine at the reported effective concentrations [13–16] for the antagonism of the histamine activity (μM level) (Table 2). Therefore, it appears unlikely that histamine is taken up into the cytosol using these histamine receptors.

To clarify the subcellular localization of the absorbed histamine, we first subdivided the cellular contents using the Percoll density gradient ultracentrifugation technique and assayed the histamine concentration of each fraction. In the BMMC of HDC(+/+) mice, the histamine was detected in the same fractions as those with β-hexosaminidase activity, which is known as one of the

Table 2. IC_{50} of the receptor antagonists and transporter inhibitors on the uptake of histamine into BMMC

Agents	IC_{50} (μM)[a]
GBR12909	>100
Maprotiline	>100
Tetrabenazine	1.25
Chlorpheniramine	75.2
Famotidine	>100
Thyoperamide	>100

a) The IC_{50} value was calculated from the mean values of triplicate assay.

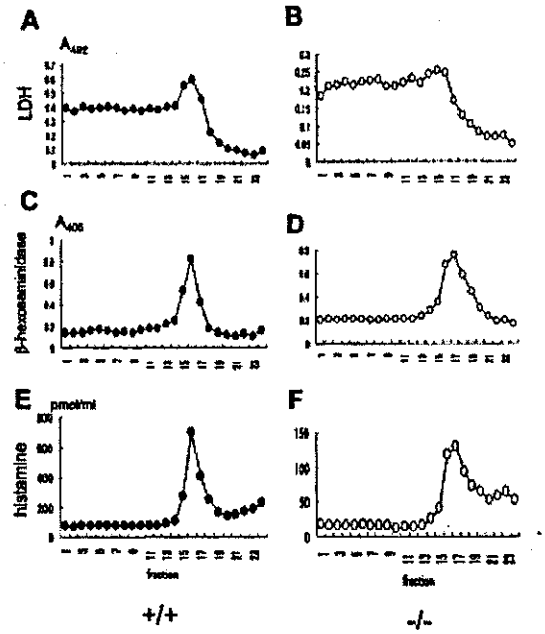

Fig. 6. Subcellular localization of the absorbed histamine assessed by fractionation on a Percoll density gradient. The contents of mildly sonicated BMMC were separated by density gradient ultracentrifugation. After the fractionation, the samples were sonicated vigorously to disrupt the organelles and assessed for LDH activity (A, B), β-hexosaminidase activity (C, D), and histamine content (E, F). BMMC were prepared from (A, C, E) HDC(+/+) and (B, D, F) HDC(–/–) mice after 16-h culture with the medium containing 100 μM histamine.

markers for secretory granules (Fig. 6C, E). In the BMMC of HDC(–/–) mice after pretreatment with 100 μM histamine-containing medium for 16 h, the histamine was detected again in the same fractions as those of the β-hexosaminidase activity (Fig. 6D, F). In other words, histamine was detected in the secretory granule fractions in the BMMC of HDC(+/+) mice and HDC(–/–) mice incubated with histamine. On the other hand, the activity of LDH, known as one of the cytosolic enzymes, was distributed from the surface fraction to the secretory granule fraction in HDC(+/+) and histamine-treated HDC(–/–) mice mast cells (Fig. 6A, B).

2.5 The release of absorbed histamine from the mast cells

To assess the functional contribution of absorbed histamine, we designed a releasing study with a physiological stimulation. The BMMC of HDC(–/–) mice were incubated with the histamine-supplemented medium for 16 h, sensitized with anti-DNP IgE, and stimulated with DNP-HSA antigen. The amounts of histamine and

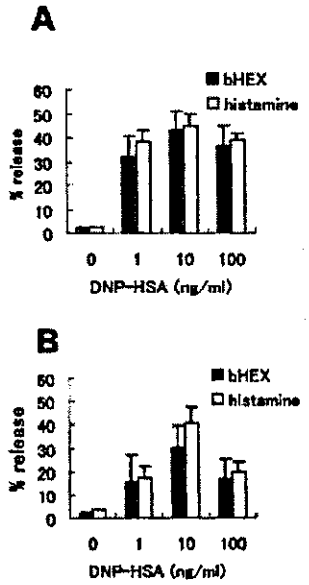

Fig. 7. The profile of histamine released by allergic stimulation from the BMMC from HDC(+/+) mice (A) and HDC(–/–) mice (B) pretreated with histamine. The cells were sensitized with anti-DNP IgE antibody and challenged with DNP-HSA antigen. The released β-hexosaminidase (bHEX) and histamine were expressed as % release against the concentration of the antigen. The culturing condition of BMMC from HDC(–/–) mice with histamine was as described in the legends to Fig. 3.

β-hexosaminidase secreted into the medium and inside the cells were measured and expressed as the % release. The maximal release of histamine and β-hexosaminidase was attained at the same concentration of DNP-HSA (10 ng /ml) in both types of mice. At this optimal concentration, 45% of the histamine and 43% of the β-hexosaminidase were released from the HDC(+/+) BMMC and 41% of the histamine and 30% of the β-hexosaminidase were released from the HDC(–/–) BMMC (Fig. 7A, B). These release profiles suggest that the absorbed histamine in the HDC(–/–) mice mast cells is stored exclusively in the secretory granules and released in the same manner as that from the wild-type mast cells.

3 Discussion

In this report we demonstrated that histamine is the mediator of plasma extravasation in the PCA reaction. The plasma extravasation in the immediate type of skin allergic reaction has been shown to be mediated by histamine, serotonin, bradykinin, leukotriene C4 [17], Neuropeptide Y [18], and vascular endothelial growth factor [19–21]. The failure of the evoked extravasation reaction

by the mast cell secretague compound 48/80 and in the PCA test in the HDC(–/–) mice on an L diet suggested histamine as the primary effector for plasma extravasation in the immediate-type allergic skin reaction. However, we cannot dismiss the possibility that other mediators, such as proteases, which may rely on the presence of histamine for their function or synthesis, could be the effectors of extravasation. We observed previously that the amounts of mouse mast cell protease (MMCP)-4, MMCP-5 and mast cell carboxypeptidase A (MC-CPA) were decreased in the peritoneal mast cells of HDC(–/–) mice [11]. Therefore, we confirmed again that there were no gross changes in the MMCP-4, MMCP-5 and MC-CPA levels (data not shown) and in the electron microscopic examination after 7 days feeding of L+HA diet. A possible effect of other mediators and the histamine deficiency on the binding efficacy of IgE receptors, and thus on the response, of mast cells should also be considered. To exclude these possibilities, it was important to design a "rescue" experiment, in which the absorbed histamine from the digestive tract would be taken up into the mast cell secretary granules. The BMMC prepared from HDC(–/–) mice took up histamine from the histamine-supplemented culture medium and released that histamine upon allergic stimulation. Although the levels of histamine were significantly reduced in the BMMC from HDC(–/–) mice (136.3±46.4 and 6.09±1.28 pmol/10^6 cells from +/+ and –/– mice BMMC, respectively n=4), the levels of serotonin were similar in both genotypes (18.6±3.6 and 15.5±2.8 nmol/10^6 cells from +/+ and –/– mice BMMC, respectively n=5). Therefore, it is highly possible that histamine *per se* is the primary effector for extravasation in the PCA reaction.

Exposure to a high amount of histamine causes protein kinase C-independent receptor desensitization [22]. Here, we suggest that this was reflected also in the results of L+HA diet, since exposure to high exogenous histamine induces a transitional disappearance of reactivity to histamine. This ability was restored 4 days after the animals were transferred to the L diet. The reaction suggests that the L+HA diet resulted in the uptake and storage of exogenous histamine in mast cells of the skin of HDC(–/–) mice, which originally lacked endogenous histamine. This also suggests that the source of the histamine in the granules is not only synthesis but also absorption from the environment.

To assess the DTH skin reaction, we prepared a CH model by applying trinitrochlorobenzene (TNCB) onto the ears of mice and measured the skin thickness of challenged ear pinna. The thickness of the ears was not affected by the histamine deficiency, suggesting that the overall role of histamine in delayed-type allergic skin reactions is not very significant. Belsito et al. [23] reported that intraperitoneal administration of an H2 antagonist, cimetidine, augmented the CH reactions. Because this augmentation was observed only when cimetidine was administered at the time of sensitisation, they suggested that the effect might be related to a cimetidine-induced inhibition of the induction of suppressor T cells, which has been reported in an *in vitro* experiment [24], at the time of sensitisation. The discrepancy between the present reaction and the reaction using an H2 antagonist could be explained by the activity of the other histamine receptors. For instance, stimulation of the H1 receptor resulted in an enhancement of *in vitro* mitogen-stimulated T cell proliferation [25] and the H1 and H2 receptors are expressed fairly exclusively in Th1 and Th2 T cells, respectively [26]. These apparent counteractions of the H1 receptor to the H2 receptor might explain the observed overall response. Other receptors including H3 and H4 might be involved in this reaction.

The uptake of the histamine into the mast cell granules involves transport through two different kinds of membranes. The first is the plasma membrane through which transport is mediated by yet unidentified transporter(s) and the second is the vesicular membrane. The second transport system is thought to include at least the VMAT2, because the BMMC from the VMAT2 knockout mice showed reduced release of histamine [12]. The second transport system (vesicular membrane transport system) should be more efficient than the first trans-plasma membrane system, because we detected high levels of histamine in the granular fraction but not in the cytosolic fraction. Therefore, once histamine has been absorbed by the mast cell, it is transported into the secretory granules quite rapidly. It was reported that the K_m value of VMAT2 for histamine is about 24 μM [27], which is a smaller value than those observed in our experiment (90 μM for the high-affinity regression line and 1.6 mM for the low-affinity regression line). Assuming that the vesicular transport is conducted mainly by VMAT2, it is not surprising that we detected little histamine in the cytosol fraction because the total efficiency of the transport in our experiments was much lower than that of the VMAT2 transport system. Therefore, the overall velocity of histamine absorption in BMMC appears to be controlled by the plasma membrane transport system.

We can hypothesize that the re-uptake is conducted by the endocytosis system; namely, histamine binds to histamine receptor(s) on the cell membrane and is taken in by the endocytotic pathway. From our results the three histamine receptors (H_1, H_2 and H_3) did not appear to participate in this system, because histamine receptor antagonists did not affect the absorption of histamine

into the secretory granules (Table 2). Therefore, the possibility that histamine receptors are involved in a receptor-mediated endocytotic pathway is unlikely.

From the Rosenthal-Scatchard plot, we could deduce two regression lines. We think that the concentration of the histamine covered by the low-affinity regression line is too high for a normal physiological situation ([histamine] >1 mM). In a model of systemic anaphylaxis, the plasma histamine concentration reached 5 μM at most (unpublished data). However, because the mast cell is the cell that releases histamine, the concentration may reach the mM level in the mast cell's microenvironment, and in that case, the low-affinity transporter may work. Histamine may be absorbed actively when the environmental histamine concentration is low but absorbed passively when the concentration exceeds the mM level.

The effect of temperature on the absorption of ^{3}H-labeled histamine was assessed under physiological conditions, *i.e.* 37°C, and at 0°C. The cells absorbed practically no histamine into the granules at 0°C, suggesting that the absorption system at a lower histamine concentration is an energy-demanding process rather than one of passive transport. This temperature dependency is reported to be one of the characteristics of the neurotransmitter uptake system [28, 29].

To determine the role of histamine, earlier studies involved the injection of HDC blockers such as α-FMH into animals. Even though α-FMH significantly decreased the level of histamine in various organs, it was difficult to achieve complete and long-lasting elimination of histamine *in vivo*. Here we demonstrated that the targeted deletion of the *HDC* gene provides a unique *in vivo* and *in vitro* model of histamine deficiency. Studies using HDC(–/–) mice will enable a detailed understanding of the role of histamine in various physiological and pathological processes.

4 Materials and methods

4.1 Mice

The generation of the HDC knockout mice was described previously [11]. The experiments were performed on 8–12-week-old male 129/Sv and CD1 congenic background mice. The HDC(+/+) and HDC(–/–) mice were chosen from littermates and compared. The low concentration histamine-containing (L) diets were purchased from commercial sources (Ver. 3 from Nihon Nosan Kogyo K.K., Yokohama, Japan). The histamine content of the L diet is 1 nmol/g diet. The histamine supplemented (L+HA) diet was made from the L diet by adding 80 μmol histamine/g diet. Mice were kept under L diet at least for 7 days before experiments except when stated otherwise.

4.2 Measurement of histamine content

The mice were anesthetized by inhalation of diethylether and transcardially perfused with heparinized saline. The histamine content and HDC activity of the organs were measured using HPLC-fluorometric system as described [30]. Briefly, for the histamine assay, organs were homogenized in 10 volumes of 3% perchloric acid containing 5 mM sodium EDTA by a Polytron homogenizer (Kinematica, Lucern, Swizerland) and centrifuged at 10,000×g for 30 min at 4°C. An aliquot of 50 μl of the supernatant was injected into the HPLC system.

4.3 HDC activity assay

For the HDC activity measurement, organs were sonicated for 20 s in 10 volumes of HDC reaction buffer (0.1 M potassium phosphate buffer pH 6.8 containing 0.2 mM dithiothreitol, 0.01 mM pyridoxal 5'-phosphate, 1% polyethylene glycol, M_r=300, and 100 μg/ml phenylmethylsulfonyl fluoride), and centrifuged at 10,000×g for 15 min at 4°C. The supernatant containing HDC protein was dialyzed overnight against the HDC reaction buffer. After a brief centrifugation, an aliquot of the supernatant was incubated with 1 ml of HDC reaction buffer containing 0.25 mM L-histidine for 2 h at 37°C. The reaction was stopped by adding 40 μl 6.2 M perchloric acid. After a brief centrifugation, the histamine content of the supernatant was measured as described above. The HDC activity was expressed as the amount of histamine formed per min per mg of protein. Protein was measured with the protein assay system (Bio-Rad, Tokyo, Japan).

4.4 Skin reactions

After the intravenous injection of Evans' blue solution, the mice were further injected with 1 μg histamine or 0.3 μg compound 48/80 (Sigma) subcutaneously into the ear. After 10 min, the mice were killed and the skin was removed for observation.

For the PCA reaction, the ears were injected with 25 ng anti-DNP IgE (Sigma). After 24 h, 60 μg DNP-HSA (HAS, Sigma) in Evans' blue solution were injected intravenously. The mice were killed 30 min after injection of the antigen. The amount of the dye extracted from the ear was determined from the absorbency at 620 nm.

To produce the CH model, mice were sensitized first on day 0 by applying 50 μl of 5% TNCB (King's Laboratory Inc., Blythewood, SC) diluted in acetone and olive oil (4:1) to the shaved dorsal neck region. On day 7 after sensitization, groups of 12 mice were challenged by applying 10 μl of the 1% TNCB solution described above to the dorsal surface of

the right ear pinna. Immediately prior to and at the indicated times after challenge, the thickness of the ear was measured using a spring-loaded engineer's micrometer (Mitutoyo, Tokyo, Japan). Ear swelling data represent the values of the ear thickness obtained at the various time points of each individual animal minus the thickness prior to the challenge.

4.5 Histology

Animals were killed 30 min or 24 h after PCA reaction. Ears were fixed in 10% formalin for 2–3 days, and processed for paraffin embedding. Tissues were cut perpendicular to the longitudinal direction of the ear. The tissue sections (4 μm) were stained with H&E and mounted.

For the peritoneal cell staining, 5 ml phosphate-buffered saline was injected into the peritoneal cavity and after slight massage it was collected and fixed in Karnovsky's, embedded in epoxy resin and analyzed using an electron microscope.

4.6 Histamine uptake in BMMC

Mouse BMMC were prepared as previously described [31], and suspended in Krebs buffer at 10^6 cells/ml buffer. To compare the uptake of histamine into BMMC from wild-type and knockout mice, we used ^{3}H-labeled histamine and measured the intracellular activity basically according to the described method [32]. [^{3}H]Histamine dihydrochloride (20 μl, 1 mCi/ml; 30–60 Ci/mmol; Amersham Pharmacia Biotech) was added into the culture medium and incubated at 0°C or 37°C for various periods. The uptake reaction was terminated by filtration through glass filters (Whatmann GF/C) using a M24S Brandel cell harvester, followed by washing with ice cold, isotonic NaCl solution for 10 s. The filters were counted in 3 ml of Aquasol scintillation fluid.

4.7 Subcellular localization of the absorbed histamine in BMMC

We fractionated the intracellular content using density-gradient centrifugation as described, with a minor modification [33]. BMMC were suspended in disruption buffer (0.25 M sucrose/10 mM Hepes pH 7.2) at 10^7 cells/ml in a Pyrex glass tube and gently sonicated in the bath sonicator (BRANSONIC Model 2210J) for 30 s at room temperature. The supernatant after the centrifugation at 1,500×g for 10 min was layered onto 20 ml of 48% (v/v) Percoll (Amersham Pharmacia Biotech) in the disruption buffer and centrifuged at 60,000×g for 55 min to fractionate the cellular content. One milliliter of each fraction was collected from the top downward and sonicated vigorously to disrupt the organelles. Each sample was assessed for LDH (LDH Cytotoxicity Detection Kit, Takara), β-hexosaminidase activity, and histamine content.

4.8 Histamine release assay in histamine-pretreated HDC(–/–) BMMC

BMMC from HDC(–/–) mice were incubated in the presence of 100 μM histamine at 37°C for 2 h before the degranulation assay. Cells (10^6) were sensitized with 1 μg/ml anti-DNP IgE for 30 min at 37°C; excess IgE was removed by centrifugation and the supernatant was discarded. Cells were then challenged with 1–100 ng/ml DNP-HSA for 30 min at 37°C. Intracellular histamine and released histamine were measured using an HPLC fluorometric system as described [34]. Degranulation was assayed by measuring the activity of the granular enzyme β-hexosaminidase in the supernatant (Sup) and cell pellet (Pel) using *p*-nitrophenyl-N-acetyl-β-D-glucosamine as substrate as described [35]. The % release was calculated according to the following formula: [Sup/(Sup + Pel)]×100.

4.9 Pharmacological intervention of histamine uptake in HDC(–/–) BMMC

To assess whether the uptake system is mediated via histamine receptor(s) or vesicular transporter, we pretreated the cells with histamine receptor antagonists, D-chlorpheniramine (Sigma), famotidine (Sigma), and thioperamide (Tocris, Bristol, GB); or transporter inhibitors, the VMAT-2 inhibitor tetrabenazine (Fluka, Buchs Switzerland), dopamine transporter inhibitor GBR 12909 (Tocris), and noradrenaline reuptake inhibitor maprotiline hydrochroride (Tocris) for 5 min, and followed the same protocol described above. To determine the concentration of compounds needed to inhibit histamine transport by 50% (IC_{50}), increasing concentrations (1–100 μM) of each agent were added to the reaction solution.

Acknowledgements: The authors are grateful to Dr. Yuko Sugita for her expertise in the experiments of IgE-mediated PCA. This work was supported by grants-in-aid form the Ministry of Education, Science and Culture of Japan and grants form the Mochida Memorial Foundation for Medical and Pharmaceutical Research and the Kanae Foundation for Life and Socio-Medical Science.

References

1 **Middleton, E. J., Reed, C. E., Ellis, E. F., Adkinson, N. F. J., Yunginger, J. W. and Busse, W. W.,** *Allergy*, 5th edn. Mosby, St. Louis 1998.

2 **Cooper, K. D.,** Atopic dermatitis: recent trends in pathogenesis and therapy. *J. Invest. Dermatol.* 1994. **102:** 128–137.

3 **Artuc, M., Hermes, B., Steckelings, U. M., Grutzkau, A. and Henz, B. M.,** Mast cells and their mediators in cutaneous wound healing-active participants or innocent bystanders? *Exp. Dermatol.* 1999. **8:** 1–16.

4 **Zhao, X., Ma, W., Das, S. K., Dey, S. K. and Paria, B. C.,** Blastocyst H(2) receptor is the target for uterine histamine in implantation in the mouse. *Development* 2000. **127:** 2643–2651.

5 **Dy, M., Arnould, A., Lemoine, F. M., Machavoine, F., Ziltener, H. and Schneider, E.,** Hematopoietic progenitors and interleukin-3-dependent cell lines synthesize histamine in response to calcium ionophore. *Blood* 1996. **87:** 3161–3169.

6 **Cricco, G. P., Davio, C. A., Martin, G., Engel, N., Fitzsimons, C. P., Bergoc, R. M. and Rivera, E. S.,** Histamine as an autocrine growth factor in experimental mammary carcinomas. *Agents Actions* 1994. **43:** 17–20.

7 **Hellstrand, K., Brune, M., Naredi, P., Mellqvist, U. H., Hansson, M., Gehlsen, K. R. and Hermodsson, S.,** Histamine: a novel approach to cancer immunotherapy. *Cancer Invest.* 2000. **18:** 347–355.

8 **Yamamoto, J., Yatsunami, K., Ohmori, E., Sugimoto, Y., Fukui, T., Katayama, T. and Ichikawa, A.,** cDNA-derived amino acid sequence of L-histidine decarboxylase from mouse mastocytoma P-815 cells. *FEBS Lett.* 1990. **276:** 214–218.

9 **Hill, S. J.,** Distribution, properties, and functional characteristics of three classes of histamine receptor. *Pharmacol. Rev.* 1990. **42:** 45–83.

10 **Watanabe, T., Yamatodani, A., Maeyama, K. and Wada, H.,** Pharmacology of alpha-fluoromethylhistidine, a specific inhibitor of histidine decarboxylase. *Trends Pharmacol. Sci.* 1990. **11:** 363–367.

11 **Ohtsu, H., Tanaka, S., Terui, T., Hori, Y., Makabe-Kobayashi, Y., Pejler, G., Tchougounova, E., Hellman, L., Gertsenstein, M., Hirasawa, N., Sakurai, E., Buzas, E., Kovacs, P., Csaba, G., Kittel, A., Okada, M., Hara, M., Mar, L., Numayama-Tsuruta, K., Ishigaki-Suzuki, S., Ohuchi, K., Ichikawa, A., Falus, A., Watanabe, T. and Nagy, A.,** Mice lacking histidine decarboxylase exhibit abnormal mast cells. *FEBS Lett.* 2001. **502:** 53–56.

12 **Travis, E. R., Wang, Y. M., Michael, D. J., Caron, M. G. and Wightman, R. M.,** Differential quantal release of histamine and 5-hydroxytryptamine from mast cells of vesicular monoamine transporter 2 knockout mice. *Proc. Natl. Acad. Sci. USA* 2000. **97:** 162–167.

13 **van der Goot, H. and Timmerman, H.,** Selective ligands as tools to study histamine receptors. *Eur. J. Med. Chem.* 2000. **35:** 5–20.

14 **Leurs, R., Brozius, M. M., Smit, M. J., Bast, A. and Timmerman, H.,** Effects of histamine H1-, H2- and H3-receptor selective drugs on the mechanical activity of guinea-pig small and large intestine. *Br. J. Pharmacol.* 1991. **102:** 179–185.

15 **Krielaart, M. J., Veenstra, D. M. and van Buuren, K. J.,** Mechanism of action of H2-antagonists on histamine- or dimaprit-stimulated H2-receptors of spontaneously beating guinea-pig atrium. *Agents Actions* 1990. **31:** 23–35.

16 **Leurs, R., Tulp, M. T., Menge, W. M., Adolfs, M. J., Zuiderveld, O. P. and Timmerman, H.,** Evaluation of the receptor selectivity of the H3 receptor antagonists, iodophenpropit and thioperamide: an interaction with the 5-HT3 receptor revealed. *Br. J. Pharmacol.* 1995. **116:** 2315–2321.

17 **Kanaoka, Y., Maekawa, A., Penrose, J. F., Austen, K. F. and Lam, B. K.,** Attenuated zymosan-induced peritoneal vascular permeability and IgE-dependent passive cutaneous anaphylaxis in mice lacking leukotriene C4 synthase. *J. Biol. Chem.* 2001. **276:** 22608–22613.

18 **Naveilhan, P., Hassani, H., Lucas, G., Blakeman, K. H., Hao, J. X., Xu, X. J., Wiesenfeld-Hallin, Z., Thoren, P. and Ernfors, P.,** Reduced antinociception and plasma extravasation in mice lacking a neuropeptide Y receptor. *Nature* 2001. **409:** 513–517.

19 **Carmeliet, P., Moons, L., Luttun, A., et al.,** Synergism between vascular endothelial growth factor and placental growth factor contributes to angiogenesis and plasma extravasation in pathological conditions. *Nat. Med.* 2001. **7:** 575–583.

20 **Thurston, G., Rudge, J. S., Ioffe, E., Zhou, H., Ross, L., Croll, S. D., Glazer, N., Holash, J., McDonald, D. M. and Yancopoulos, G. D.,** Angiopoietin-1 protects the adult vasculature against plasma leakage. *Nat. Med.* 2000. **6:** 460–463.

21 **McDonald, D. M., Thurston, G. and Baluk, P.,** Endothelial gaps as sites for plasma leakage in inflammation. *Microcirculation* 1999. **6:** 7–22.

22 **Zamani, M. R., Dupere, J. R. and Bristow, D. R.,** Receptor-mediated desensitisation of histamine H1 receptor-stimulated inositol phosphate production and calcium mobilisation in GT1-7 neuronal cells is independent of protein kinase C. *J. Neurochem.* 1995. **65:** 160–169.

23 **Belsito, D. V., Kerdel, F. A., Potozkin, J. and Soter, N. A.,** Cimetidine-induced augmentation of allergic contact hypersensitivity reactions in mice. *J. Invest. Dermatol.* 1990. **94:** 441–445.

24 **Sahasrabudhe, D. M., McCune, C. S., O'Donnell, R. W. and Henshaw, E. C.,** Inhibition of suppressor T lymphocytes (Ts) by cimetidine. *J. Immunol.* 1987. **138:** 2760–2763.

25 **Banu, Y. and Watanabe, T.,** Augmentation of antigen receptor-mediated responses by histamine H1 receptor signaling. *J. Exp. Med.* 1999. **189:** 673–682.

26 **Jutel, M., Watanabe, T., Klunker, S., Akdis, M., Thomet, O. A., Malolepszy, J., Zak-Nejmark, T., Koga, R., Kobayashi, T., Blaser, K. and Akdis, C. A.,** Histamine regulates T cell and antibody responses by differential expression of H1 and H2 receptors. *Nature* 2001. **413:** 420–425.

27 **Merickel, A. and Edwards, R. H.,** Transport of histamine by vesicular monoamine transporter-2. *Neuropharmacology* 1995. **34:** 1543–1547.

28 **Chin, C. A. and Lam, D. M.,** The uptake and release of [3H]glycine in the goldfish retina. *J. Physiol.* 1980. **308:** 185–195.

29 **Chang, A. S., Frnka, J. V., Chen, D. N. and Lam, D. M.,** Characterization of a genetically reconstituted high-affinity system for serotonin transport. *Proc. Natl. Acad. Sci. USA* 1989. **86:** 9611–9615.

30 **Ohtsu, H., Kuramasu, A., Suzuki, S., Igarashi, K., Ohuchi, Y., Sato, M., Tanaka, S., Nakagawa, S., Shirato, K., Yamamoto, M., Ichikawa, A. and Watanabe, T.,** Histidine decarboxylase expression in mouse mast cell line P815 is induced by mouse peritoneal cavity incubation. *J. Biol. Chem.* 1996. **271:** 28439–28444.

31 **Eklund, K. K., Ghildyal, N., Austen, K. F., Friend, D. S., Schiller, V. and Stevens, R. L.,** Mouse bone marrow-derived mast cells (mBMMC) obtained in vitro from mice that are mast cell-deficient *in vivo* express the same panel of granule proteases as mBMMC and serosal mast cells from their normal littermates. *J. Exp. Med.* 1994. **180:** 67–73.

32 **Hardy, J., Cowburn, R., Barton, A., Reynolds, G., Lofdahl, E., O'Carroll, A. M., Wester, P. and Winblad, B.,** Region-specific loss of glutamate innervation in Alzheimer's disease. *Neurosci. Lett.* 1987. **73:** 77–80.

33 **Serafin, W. E., Guidry, U. A., Dayton, E. T., Kamada, M. M., Stevens, R. L. and Austen, K. F.,** Identification of aminopeptidase activity in the secretory granules of mouse mast cells. *Proc. Natl. Acad. Sci. USA* 1991. **88:** 5984–5988.

34 **Yamatodani, A., Fukuda, H., Wada, H., Iwaeda, T. and Watanabe, T.,** High-performance liquid chromatographic determination of plasma and brain histamine without previous purification of biological samples: cation-exchange chromatography coupled

with post-column derivatization fluorometry. *J. Chromatogr.* 1985. **344:** 115–123.

35 **Ortega, E., Hazan, B., Zor, U. and Pecht, I.,** Mast cell stimulation by monoclonal antibodies specific for the Fc epsilon receptor yields distinct responses of arachidonic acid and leukotriene C4 secretion. *Eur. J. Immunol.* 1989. **19:** 2251–2256.

Correspondence: Hiroshi Ohtsu, Department of Cellular Pharmacology, Tohoku University Graduate School of Medicine, 2–1 Seiryo-cho, Aoba-ku, Sendai 980–8575, Japan
Fax: +81-22-717-8058
e-mail: ohtsu@mail.cc.tohoku.ac.jp

ELSEVIER

Journal of Hepatology 36 (2002) 328–334

Journal of Hepatology

www.elsevier.com/locate/jhep

Contribution of the two Gs-coupled PGE_2-receptors EP2-receptor and EP4-receptor to the inhibition by PGE_2 of the LPS-induced TNFα-formation in Kupffer cells from EP2-or EP4-receptor-deficient mice. Pivotal role for the EP4-receptor in wild type Kupffer cells

Alexandra Fennekohl[1], Yukihiko Sugimoto[2], Eri Segi[2], Takayuki Maruyama[3], Atsushi Ichikawa[2], Gerhard P. Püschel[1,*]

[1]*Universität Potsdam, Institut für Ernährungswissenschaft, Abteilung Biochemie der Ernährung, Arthur-Scheunert-Allee 114–116, D-14558 Bergholz-Rehbrücke, Germany*

[2]*Faculty of Pharmaceutical Sciences, Kyoto University, Sakyo-ku, Kyoto 606-8501, Japan*

[3]*Discovery Research Laboratory, Minase Research Institute, ONO Pharmaceutical Co, Ltd., Osaka 618-8585, Japan*

***Background/Aims*: Prostaglandin E_2 (PGE_2) is known to inhibit the lipopolysaccharide (LPS)-induced tumor necrosis factor α (TNFα) formation in Kupffer cells via an increase in cAMP. Four receptor-subtypes have been cloned for PGE_2 so far. Two of them, the EP2-receptor and the EP4-receptor are linked to stimulatory Gs-proteins and could mediate the inhibition by PGE_2 of TNFα-formation.**

***Methods*: The significance of both receptors for PGE_2-dependent inhibition of LPS-induced TNFα-formation was studied using Kupffer cells of mice in which either one of the two receptors had been eliminated by homologous recombination.**

***Results*: The mRNAs of both receptors were expressed in wild type mouse Kupffer cells. Exogenous PGE_2 inhibited TNFα-formation in Kupffer cells lacking either EP2-receptor or EP4-receptor to a similar extent as in control cells, however, 10-fold higher PGE_2 concentrations were needed for half maximal inhibition in cells lacking the EP4-receptor than in control or EP2-receptor-deficient cells. The response to endogenous PGE_2 was blunted in EP4-receptor-deficient mice only and especially after prolonged incubation.**

***Conclusions*: The data indicate, that PGE_2 can inhibit TNFα-formation via both the EP2- and the EP4-receptor and that, however, the EP4-receptor appears to be physiologically more relevant in Kupffer cells since it conferred a high affinity response to PGE_2.**

***Keywords*: Prostanoid receptors; Liver; Cyclic AMP; Inflammation; K. o. mouse**

Received 20 March 2001; received in revised form 24 October 2001; accepted 29 October 2001

* Corresponding author. Tel.: +49-33-2008-8694; fax: +49-33-2008-8541.

E-mail address: gpuesche@rz.uni-potsdam.de (G.P. Püschel).

Abbreviations: LPS, lipopolysaccharide; IL-6, interleukin-6; PGE_2, prostaglandin E_2; TXA_2, thromboxane A_2; $PGF_{2\alpha}$, prostaglandin $F_{2\alpha}$; PGE_1, prostaglandin E_1; PGI_2, prostacyclin; NO, nitric oxide; TNFα, tumor necrosis factor α; cAMP, cyclic AMP; PGD_2, prostaglandin D_2; EP1-R, PGE_2-receptor subtype 1; EP3-R, PGE_2-receptor subtype 3; EP2-R, PGE_2-receptor subtype 2; EP4-R, PGE_2-receptor subtype 4; EP-R, PGE_2-receptor; CHO cells, Chinese hamster ovarian cells; HBSS, Hank's balanced salt solution; cDNA, complementary DNA; PCR, polymerase chain reaction; RT-PCR, reverse transcriptase-PCR.

1. Introduction

Prostanoids are involved in the regulation of hepatic functions during inflammation. They are released from non-parenchymal liver cells in response to a large array of inflammatory stimuli such as lipopolysaccharide (LPS) [1], zymosan [2], anaphylatoxins [3,4] and proinflammatory cytokines [5]. Prostanoids modulate hepatocyte functions in a paracrine mode: they influence the glucogenic activity of the hepatocyte by regulation of enzyme activity [6–9], control of the expression level of key glucogenic enzymes [10] and also indirectly via a modulation of sinusoidal blood flow [11].

0168-8278/02/20.00
PII: S0168-8278(01)00277-X

Recently, they have been shown to attenuate the IL-6-induced acute phase response of the hepatocyte after an IL-6-dependent expression of previously absent Gs-coupled prostaglandin E_2-(PGE_2-) receptors [12]. Prostanoids also modulate non-parenchymal cell functions in paracrine and autocrine modes, e.g. thromboxane A_2 (TXA_2) or prostaglandin $F_{2\alpha}$ ($PGF_{2\alpha}$) contract trans-differentiated hepatic stellate cells [13] while contraction is inhibited by PGE_1, PGE_2 or prostacyclin (PGI_2) [14,15]. The LPS-induced release of NO [16,17], reactive oxygen species, or cytokines [18] from Kupffer cells is inhibited by PGE_2. For the LPS-induced release of TNFα an autocrine feedback inhibition loop has been shown to exist [19,20]: LPS and TNFα stimulate the release of PGE_2 from Kupffer cells. PGE_2 in turn attenuates the TNFα-production via an increase in intracellular cAMP [19]. It is not known so far, which prostanoid-receptor is involved in this signaling chain.

Prostanoids exert their effects on their target cells via heptahelical transmembrane receptors. For the five prostanoids prostaglandin E_2 (PGE_2), prostaglandin $F_{2\alpha}$ ($PGF_{2\alpha}$), prostaglandin D_2 (PGD_2), prostacyclin (PGI_2) and thromboxane A_2 (TXA_2) there exist eight types of G-protein-coupled receptors [21]. Four subtypes exist for PGE_2, that are coupled to different heterotrimeric G-proteins. The EP1-receptor (EP1-R) couples to Gq, the EP3-receptor (EP3-R) couples to Gi whereas the EP2-receptor (EP2-R) and the EP4-receptor (EP4-R) couple to Gs [22]. These receptors are expressed differentially in the four principal liver cells types, i.e. hepatocytes, Kupffer cells, sinusoidal endothelial cells and hepatic stellate cells [23]. Kupffer cells express both types of Gs-coupled PGE_2-R that might possibly confer the PGE_2-mediated cAMP-dependent inhibition of TNFα-production. Therefore, the question was addressed, which of the two receptors is part of the feedback inhibition loop. Using Kupffer cell cultures isolated from mice lacking either the EP2-R or the EP4-R it was shown, that both receptors can mediate the PGE_2-dependent inhibition of LPS-induced TNFα-formation and can at least partially substitute for each other in Kupffer cells of receptor deficient mice. However, the EP4-R appeared to be physiologically more relevant.

2. Materials and methods

2.1. Materials

All materials were from commercial sources and analytical grade. Reverse transcription was primed with oligo(dT) (Pharmacia, Freiburg, Germany). PCR primers were custom synthesized by NAPS (Göttingen, Germany). Pronase E was purchased from Merck (Darmstadt, Germany). Collagenase H and DNase I were from Boehringer (Mannheim, Germany). The ELISA for TNFα was purchased from Pharmingen (San Diego, CA, USA). The radioimmunoassay for PGE_2 was from Amersham. ELISA and radioimmunoassay were carried out exactly following the instructions of the provider. LPS O55:B5 from Escherichia coli and indomethacine were from Sigma (Deisenhofen, Germany). PGE_2 was purchased from Calbiochem (Frankfurt a. M., Germany). The EP2-R-specific agonist ONO 613 and the EP4-R-specific agonist ONO 604 were generated by ONO Pharmaceutical Co, Ltd., Osaka, Japan, and the specificity was analyzed by measuring binding affinity to the respective PGE_2-receptors (EP-R) expressed in Chinese hamster ovarian (CHO) cells (Table 1). PGE_2 bound to all EP-Rs. Based on the results obtained from dose-dependency analysis, we used 1 μM of ONO613 (EP2-R agonist) and 10 nM of ONO604 (EP4-R agonist) in the present experiments. In these concentrations, the respective agonists selectively activate EP2-R and EP4-R, respectively.

2.2. Generation of EP2-R-deficient and EP4-R-deficient mice

Mice strains, that are deficient in the gene for either the EP2-R or the EP4-R, were generated by homologous recombination as described elsewhere [24,25]. The EP2-R-null and EP4-R-null mutations were individually introduced in embryonic stem cells derived from 129/Ola mice. Chimeras derived from these cells were bred with C57BL/6 mice, resulting in generation of homozygous mice. EP2-R−/− mice with a mixed background of 129/Ola and C57BL/6 were maintained in the same colony, and used for these experiments. Controls for these studies were wild-type mice derived from the same colony. Although most EP4-R−/− mice die within 3 days from complications of patent ductus arteriosus, by selective breeding on a mixed background, EP4-R−/− lines have been produced in which the ductus closes and the animals survive normally ([26], Segi E, Sugimoto Y, Ichikawa A, unpublished data). EP4-R−/− mice from these selected mixed background were used in these experiments. The genetic background of these animals consists of a mixture of 129/Ola and C57BL/6. Animals were maintained at 23°C under a 12 h light cycle, fed a normal diet and provided with water ad libitum. Treatment of the animals followed the German and Japanese Law on the Protection of Animals and was performed with permission of the state animal welfare committee.

2.3. Isolation and culture of Kupffer cells

Kupffer cells were isolated from mouse livers by pronase/collagenase perfusion. Briefly, livers were perfused in situ without recirculation first with HBSS with a flow of 10 ml/min until livers were blood-free. The flow was reduced to 5 ml/min and the liver was perfused with 25 ml HBSS containing 0.4% (w/v) pronase E, followed by perfusion with 35 ml HBSS containing 0.014% (w/v) collagenase H and 0.0014% (w/v) DNase I. The excised and disrupted liver was digested at 37°C for 10–15 min in 25 ml HBSS containing 0.1% (w/v) pronase E and 0.01% (w/v) DNase I. Kupffer cells were separated from detritus and other cells by differential centrifugation in HBSS followed by a two-step nycodenz gradient consist-

Table 1
Binding affinities of an EP2-R agonist, ONO613, and an EP4-R agonist, ONO604, to the respective EP-Rs expressed in CHO cells[a]

Receptors [^{3}H]-Ligands	EP1-R [^{3}H]-PGE_2	EP2-R [^{3}H]-PGE_2	EP3-R [^{3}H]-PGE_2	EP4-R [^{3}H]-PGE_2
PGE_2	0.018	0.038	0.005	0.0031
ONO613	>10	0.092	>10	>10
ONO604	0.61	0.28	1.5	0.0007

[a] The partially purified membrane of CHO cells expressing the respective EP-Rs was used for the [^{3}H]-PGE_2 binding assay, and the Ki value (micromolar concentrations) was calculated as shown previously [31].

ing of a cushion of 18% (w/v) nycodenz, the cell suspension containing 11% (w/v) nycodenz and a top layer of HBSS. The gradient was centrifuged for 45 min at 1000 × *g*. Kupffer cells were enriched at the interphase between 11 and 18% nycodenz, whereas hepatic stellate cells and the majority of sinusoidal endothelial cells floated on the 11% (w/v) nycodenz cushon. The Kupffer cell yield was about 26×10^6 cells/liver and did not vary significantly between control and EP2-R- or EP4-R-deficient mice. Kupffer cells were further purified by differential adhesion on tissue culture dishes, i.e. a medium change with rigid washing 6 h after plating thereby removing sinusoidal endothelial cells possibly contaminating the early culture which do not adhere under these conditions. The Kupffer cells were cultured on 24-well plates (1×10^6 cells/well) in RPMI (Gibco-BRL, Eggenstein, Germany) containing 20% (v/v) FCS (Biochrom, Berlin, Germany) and antibiotics (10 mg/ml penicillin/streptomycin, Gibco-BRL) for the times indicated prior to the experiment.

2.4. cDNA-preparation and PCR-protocols

Total RNA was isolated from cultured Kupffer cells by RNeasy (Qiagen, Hilden, Germany). cDNA was synthesized from total RNA by oligo(dT)-primed reverse transcription with Superscript II (Gibco-BRL, Eggenstein, Germany) according to the instructions of the manufacturer. PCRs were carried out in a 50 µl reaction mix containing 30 pmol of forward and reverse primer, 200 µM of each deoxyribonucleotide triphosphate (dNTPs), 3% (v/v) dimethyl sulfoxide, serial dilutions of the cDNA-preparation, 5 µl of 10 × buffer and 0.25 U ProHA-Polymerase (Eurogentec, Seraing, Belgium). The mix was subjected to the following PCR-programs: EP2-R; 3 min 95°C, 35 × (1 min 95°C, 1 min 58°C, 2 min 72°C). EP4-R; 3 min 95°C, 35 × (1 min 95°C, 1 min 61°C, 2 min 72°C). β-actin; 3 min 95°C, 35 × (1 min 95°C, 1 min 60°C, 2 min 72°C). The primer sequences were chosen from published cDNA-sequences as follows: EP2-R: Acc No.: U48858; forward primer: 498–517; reverse primer: 1117–1095. EP4-R: Acc No.: D28866; forward primer: 731–753; reverse primer: 1389–1366. β-actin: Acc No.: J00691; forward primer: 1251–1271; reverse primer: 2570–2553. The quantity and integrity of the cDNA was checked by PCR for β-actin. To compensate for the different amplification efficacy of the PCR-protocols and the different abundance of the mRNAs of the prostanoid-receptors the first dilution was adjusted relative to β-actin as follows: EP2-R and EP4-R, 2.5:1. The stocks were further diluted 1:4 and 1:16 in order to be in the linear range of the PCR. Products were separated electrophoretically on 2% (w/v) agarose gels and visualized by staining with ethidium bromide.

2.5. Stimulation of TNFα-production in Kupffer cells

For all experiments the cultured Kupffer cells were washed twice with serum-free medium.

(a) To study which of the Gs-coupled PGE_2-receptors (EP2-R or EP4-R) is involved in the PGE_2-mediated feedback inhibition of LPS-induced TNFα-formation Kupffer cells were incubated in serum-free medium in presence of E. coli lipopolysaccharide (LPS, 100 ng/ml), LPS+indomethacine (10 µM), LPS+PGE_2 (100 nM), LPS+EP2-R-specific agonist (1 µM ONO613) or LPS+EP4-R-specific agonist (10 nM ONO604). After 6 h supernatants were harvested and the TNFα-concentration was determined by ELISA.

(b) To determine the dose-dependence of the PGE_2-mediated inhibition of LPS-induced TNFα-formation Kupffer cells were cultured for 72 h prior to the addition of LPS (100 ng/ml) alone or LPS+0.1 nM PGE_2, LPS+1 nM PGE_2, LPS+10 nM PGE_2, LPS+100 nM PGE_2 and LPS+1 µM PGE_2. Culture was continued for 6 h. Then supernatants were harvested and TNFα-concentration was determined by ELISA.

(c) To analyze the time-dependence of the PGE_2-mediated inhibition of LPS-induced TNFα-formation Kupffer cells were cultured for 86, 84, 82, 80, 76, 70, 64 and 40 h prior to the addition of LPS (100 ng/ml) alone or LPS+1 µM PGE_2; culture was then continued for 2, 4, 6, 8, 12, 18, 24 and 40 h. Again supernatants were harvested and TNFα-concentration was determined by ELISA.

3. Results

3.1. Expression of EP2-R and EP4-R in mouse Kupffer cells

It has been shown previously, that both the EP2-R and the EP4-R receptor were expressed in Kupffer cells of the rat [23]. Since there appear to exist differences in prostanoid receptor distribution between rat and mouse, the presence of the EP2-R mRNA and EP4-R mRNA had to be confirmed in mouse Kupffer cells. Further more it was important to show that the disruption of the gene of either one of the Gs-coupled PGE_2-receptors did not lead to a compensatory overexpression of the remaining one. By RT-PCR it was shown that in mouse Kupffer cells, similar to rat Kupffer cells, the mRNAs of both receptors, the EP2-R and the EP4-R, were expressed (Fig. 1). The mRNA for the EP2-R was not detectable in EP2-R-deficient cells. On the other hand the EP4-R-mRNA could not be found in EP4-R-deficient cells. No compensatory overexpression of either one of the two receptor was observed in cells lacking the other. In contrast to previous findings with macrophage cell lines [27] no significant induction by LPS of either receptor was detectable (Fig. 1).

3.2. Inhibition of LPS-induced TNFα-production in Kupffer cells by PGE_2 and receptor-specific agonists

Kupffer cells from control or receptor-deficient mice did not produce significant amounts of TNFα without stimulation. Incubation of Kupffer cells with 100 ng LPS/ml over a period of 6 h resulted in an increase of TNFα in cell supernatants. LPS-stimulated TNFα-levels tended to be higher in EP4-R-deficient mice (Fig. 2). The level of endogenous PGE_2-production after stimulation of the cells with LPS was determined by measuring released PGE_2 in the supernatant after 6 h by RIA and did not differ significantly between the groups: Control cells released 5.1 ± 0.59 nmol/l PGE_2, EP2-R-deficient cells 4.22 ± 1.04 nmol/l and EP4-R-deficient cells produced 5.89 ± 0.85 nmol/l PGE_2 (data not shown). Indomethacin (100 ±M) which inhibits the endogenous LPS- and/or TNFα-stimulated PGE_2-production further enhanced the LPS-induced TNFα-formation in Kupffer cells of control and EP2-R−/− mice, yet, it had no influence on the LPS-induced TNFα-formation in EP4-R−/− cells (Fig. 2). Exogenous PGE_2 (100 nM) reduced the LPS-stimulated TNFα-formation in control cells by almost 90%. The PGE_2-dependent inhibition of the LPS-induced TNFα-formation was almost equally effective in EP2-R-deficient cells, however, it was clearly less effective in EP4-R-deficient cells where it reduced TNFα-formation by merely 50% (Fig. 2). To exclude that the EP2-R can inhibit the LPS-induced TNFα-formation in EP4-R−/− Kupffer cells only, the inhibition of the LPS-induced TNFα-formation was studied with agonists, which were specific for either the EP2-R (ONO613) or the EP4-R (ONO604) (Table 1). The EP2-

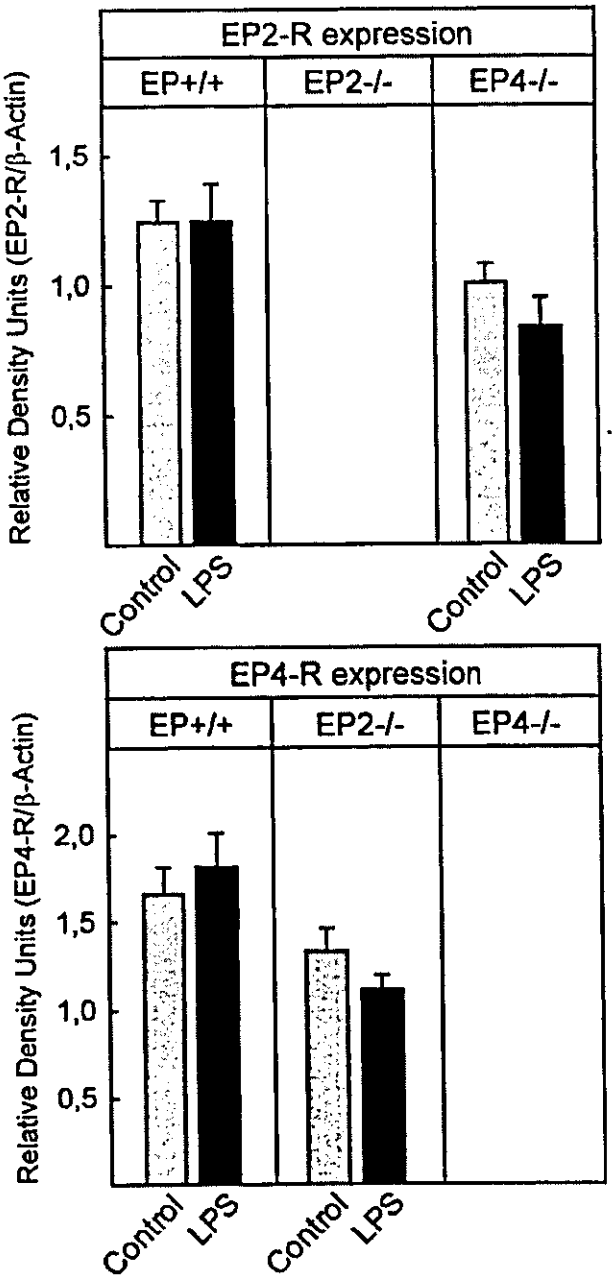

Fig. 1. mRNA-Expression of the EP2-R and EP4-R in Kupffer cells of control mice and EP2-R-deficient and EP4-R-deficient mice. Kupffer cells were isolated from control, EP2-R- and EP4-R-deficient mice by combined pronase/collagenase perfusion. They were cultured for 72 h in RPMI medium containing 20% (v/v) FCS. Total RNA was isolated from cultivated Kupffer cells by affinity chromatography and used as a template for oligo(dT)-primed cDNA synthesis. Thirty-five cycles of PCR were performed with specific primers for the EP2-R and EP4-R or β-actin with serial dilutions of cDNAs to ensure that the PCR reaction was not saturated. The intensity of the bands of the EP2-R or EP4-R amplificate was quantified densitometrically and compared with the intensity of the corresponding β-actin bands. Values are means ± SEM of the relative intensities; $n = 18$ in 6 cDNA-preparations from independent cell culture experiments for control (EP+/+) cells and $n = 9$ in 3 cDNA-preparations from independent cell culture experiment for EP2−/− and EP4−/−, respectively.

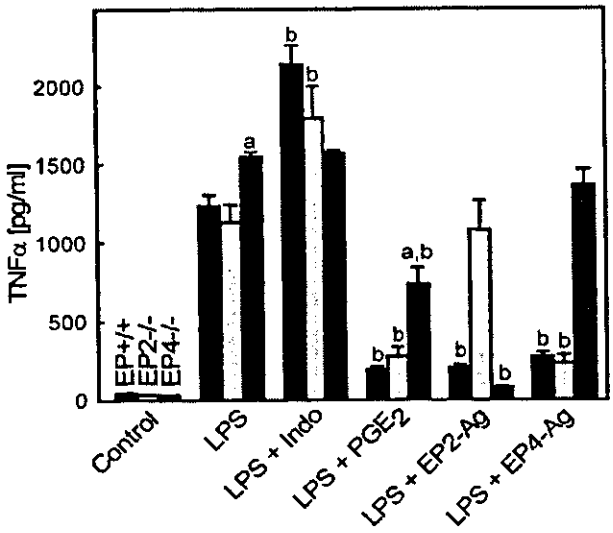

Fig. 2. Inhibition by PGE_2 of the LPS-induced TNFα-formation in Kupffer cells from control and EP2-R-deficient or EP4-R-deficient mice. Kupffer cells were isolated from control mice, EP2-R-deficient mice or EP4-R-deficient mice as described in the legend to Fig. 1. They were cultured for 72 h in RPMI medium containing 20% (v/v) FCS and then stimulated with LPS (100 ng/ml), LPS+indomethacine 10 μM (Indo), LPS+PGE_2 (100 nM), LPS+1 μM of the EP2-R-agonist ONO613 (EP2-Ag) or, LPS+10 nM of the EP4-R-agonist ONO604 (EP4-Ag) in serum free medium for 6 h. TNFα-concentration was determined in the cell culture supernatants by ELISA. Values are means ± SEM of 8 (EP2−/− or EP4−/− cells) to 24 (control cells) determinations in four to eight independent experiments. Statistics: Student's *t*-test for unpaired samples; (a) significantly different from EP-R+/+ mice under identical conditions; and (b) significantly different from LPS-stimulated cells of the same group.

specific agonist ONO613 and the EP4-specific agonist ONO604 at concentrations, which did not activate the EP4-R or the EP2-R, respectively, inhibited the LPS-induced TNFα-formation in control cells to a similar extent as PGE_2. As expected, the EP2-R agonist failed to inhibit TNFα-production in EP2-R-deficient cells while the EP4-R agonist did not attenuate TNFα-formation in EP4-R-deficient cells (Fig. 2).

3.3. Dose and time dependence of the inhibition by PGE_2 of LPS-induced TNFα-formation

The EC50 (Fig. 3) for the inhibition by exogenous PGE_2 of TNFα-formation was about 10 nM in control or EP2-R−/− cells. A 10-fold higher EC50 of about 100 nM was determined in EP4-R−/− cells. These results showed that both receptors independently of each other can mediate an attenuation of the LPS-induced TNFα-formation in Kupffer cells. Moreover the findings indicate that the EP4-R might be responsible for the inhibition of LPS-induced TNFα-formation at low PGE_2-concentrations, as they are generated by the Kupffer cells themselves. The EP4-R thus might be responsible for a physiological high affinity response to PGE_2, whereas the EP2-R can only inhibit the LPS-induced

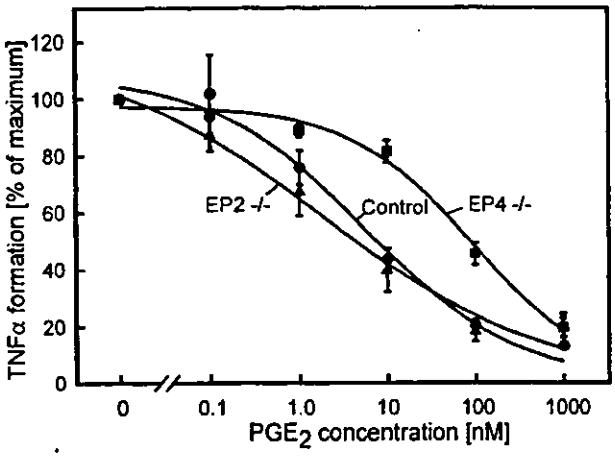

Fig. 3. Dose dependence of the inhibition by PGE_2 of the LPS-induced TNFα-formation in Kupffer cells from control and EP2-R-deficient or EP4-R-deficient mice. Kupffer cells were isolated and cultured for 72 h as described in legend to Fig. 1. They were then stimulated for 6 h in serum free medium with LPS (100 ng/ml) ± PGE_2 in the concentration indicated. TNFα-concentration was determined in the cell culture supernatants by ELISA. Values are expressed as % of the TNFα-concentration in the supernatants of LPS-stimulated cells. They are means ± SEM of nine to 57 determinations in three to 19 independent experiments. A total of 100% values ± SD are 1393 ± 436, 1785 ± 848 and 1936 ± 603 pg/ml for control, EP2−/− and EP4−/− cells, respectively.

TNFα-formation at higher concentrations and thus mediated a low affinity response.

The EP4-R shows rapid agonist desensitization whereas the EP2-R does not [28]. It was therefore assumed, that the EP4-R might be responsible for an early response to PGE_2 while the EP2-R mediates the PGE_2-effects in the late phase. The time course of the TNFα-production argues against this hypothesis (Fig. 4). TNFα-concentrations in the supernatants of Kupffer cells increased towards a maximum at 8 h and then gradually declined towards basal levels in control and EP2-R-deficient cells. Unexpectedly TNFα-levels remained elevated in EP4-R-deficient cells, indicating that endogenous PGE_2 inhibited the TNFα-formation principally via the EP4-R also after prolonged exposure. Exogenous PGE_2 inhibited the TNFα-formation equally well over the entire time range studied.

4. Discussion

We previously found that in freshly isolated rat Kupffer cells the EP2-R mRNA was more abundant than in any other liver cell type [23]. In addition, the EP2-R mRNA has been shown to be present in monocytes/macrophages of other origin and in monocyte/macrophage cell lines [27,29] where it was induced to a much larger extent by LPS than the EP4-R [27]. Therefore it was assumed, that mainly the EP2-R might be involved in the regulation of the LPS-induced TNFα-formation in Kupffer cells. In spite of the information suggesting a dominant role of EP2-R in Kupffer cells, the data of the present study showed, that the two Gs-coupled PGE_2-receptors, the EP2-R and the EP4-R, are able to substitute for each other in mediating the PGE_2-dependent inhibition of the LPS-induced TNFα-formation in Kupffer cells. In contrast to the expectation, the data rather favor the EP4-R being the physiologically more relevant receptor in this feedback inhibition loop.

A direct comparison of the mRNA levels of the EP2-R- and EP4-R-mRNA performed in this study by RT-PCR showed that, in contrast to freshly isolated [23] or cultured (Fennekohl, unpublished data) rat Kupffer cells, mouse Kupffer cells showed a similar signal intensity in the PCRs for both Gs-coupled receptors, suggesting, that unlike in rat Kupffer cells there appeared not to be a predominance of the EP2-R (Fig. 1: [23]). In contrast to findings in macrophage cell lines [27] no significant induction of the EP2-R-mRNA by LPS was detectable.

4.1. EP4-R-mediated inhibition of LPS-induced TNFα-formation at early time points

The PGE_2-dependent inhibition of the LPS-induced TNFα-formation was maintained in Kupffer cells of mice lacking either one of the two receptors (Fig. 2). Stimulation of either receptor with subtype-specific agonists was sufficient to inhibit TNFα-formation to a similar extent as receptor saturating concentrations of PGE_2 that does not display subtype specificity (Fig. 2). This is in line with similar findings in gingival fibroblasts [30]. However, the concentra-

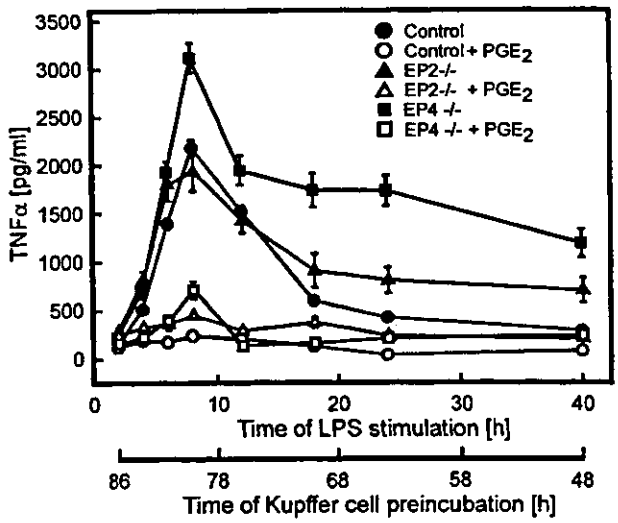

Fig. 4. Time dependence of the inhibition by PGE_2 of the LPS-induced TNFα-formation in Kupffer cells from control and EP2-R-deficient or EP4-R-deficient mice. Kupffer cells were isolated and cultured for 48–86 h as described in legend to Fig. 1. They were then stimulated for the times indicated in serum free medium with LPS (100 ng/ml) ± PGE_2 (1 μM). After a total culture time of 88 h in all cells supernatants were sampled for determinations of the TNFα-concentration by ELISA. Values are are means ± SEM of nine to 57 determinations in three to 19 independent experiments.

tions of PGE_2 found in the supernatants of LPS-stimulated Kupffer cells due to endogenous production, were not receptor-saturating. These low concentrations of about 5 nM were in the range of the EC50 found for the EP4-R (about 10 nM, Fig. 3) and were 20-fold lower than the EC50 of the EP2-R (about 100 nM, Fig. 3) that correspond to the Kd values of the cloned receptors reported previously [31]. In line with a pivotal role of the EP4-R in the feedback inhibition in response to low endogenous PGE_2-concentrations, elimination of the EP4-R but not the EP2-R resulted in an increase of the LPS-induced TNFα-formation in comparison to control cells (Fig. 2) and inhibition of endogenous PGE_2-formation augmented LPS-induced TNFα-formation only in Kupffer cells expressing the EP4-R after 6 h of LPS-stimulation (Fig. 2).

For rat Kupffer cells it was shown that at this early stage after LPS-stimulation endogenous PGE_2 can inhibit TNFα-formation at transcriptional level by inhibition of LPS-induced NFκB-activation via an elevation of intracellular cAMP [32,33]. In contrast in human monocytes cAMP inhibits TNFα-production through a posttranscriptional mechanism [34], whereas cAMP has no inhibitory effect on TNFα-mRNA-levels or NFκB-activation.

In summary the results indicate that both Gs-coupled receptors, the EP2-R and the EP4-R can confer the PGE_2-mediated inhibition of the LPS-induced TNFα-formation. However the EP4-R seems to play a pivotal role for the inhibition of LPS-induced TNFα-formation at low endogenous PGE_2-concentrations. It is assumed that the EP4-R serves as a high affinity receptor in the first line whereas the EP2-R with its lower affinity becomes relevant only at sufficiently high PGE_2-concentration. However, the parallel action of both receptors might be required to obtain full inhibition of the LPS-induced TNFα-formation also at low endogenous PGE_2-concentrations, as indicated by the failure of TNFα-levels to return to control levels at late time points in Kupffer cells missing either receptor (Fig. 4).

4.2. EP4-R-mediated inhibition of LPS-induced TNFα-formation at late time points

The TNFα-concentration in Kupffer cell supernatants declined after a maximum at 8 h. Since no plateau was reached a degradation or sequestration, e.g. by soluble TNFα-receptor, of previously formed TNFα must have occurred besides a reduction of the LPS-induced TNFα-de novo-synthesis. Endogenous PGE_2 might modulate the decline of TNFα-levels at late time points either by inhibiting TNFα-synthesis or by increasing its degradation or sequestration. If endogenous PGE_2 also inhibits LPS-induced TNFα-formation in Kupffer cells after long exposure on transcriptional level is not known. The influence of posttranscriptional mechanisms on decreased TNFα-levels at later time points cannot be ruled out. It was shown that PGE_2 upregulates soluble 55- and 75-kDa TNF-receptor in human monocytic THP-1 cells, whereas the mRNA-levels of both receptors remained unchanged [35]. By this shedding of TNF-receptors TNFα in the supernatant might be neutralized and TNFα-levels as detected by ELISA decrease due to the interference of the soluble receptor with the capture antibody.

One clue to the puzzle that Kupffer cells express two receptors for the same ligand PGE_2 that are coupled to the same intracellular signal chain appeared to be the different susceptibility of the two receptors to agonist-induced desensitization. The EP4-R does show rapid agonist-induced desensitization whereas the EP2-R does not [28,31]. This would imply, that the EP4-R were active principally at early stages of the exposure of Kupffer cells to the ligand whereas the EP2-R were more important at later stages, when the EP4-R is desensitized. The results of the current study do not support such an hypothesis (Fig. 4). Both EP2-R- and EP4-R-deficient Kupffer cells were sensitive to exogenous PGE_2 over the total range of 48 h. No desensitization was observed in the EP2-R-deficient cells. Rather, endogenous PGE_2 seemed to be less effective in inhibiting the TNFα-formation at any time points in EP4-R-deficient cells, pointing towards a predominant function of the EP4-R even after long exposure to endogenous PGE_2.

It appears unreasonable to assume that the two types of receptors with different affinities are merely a double save guard. Differential regulation of their genes at various stages of macrophage-like cell function might give an indication. Indeed, the resident macrophages isolated from peritoneal cavity express only EP4-R without any stimulations, but once exposed to LPS, they do not express EP4-R any more (Sugimoto Y, Katsuyama M, Segi E, Ikegami R, Ichikawa A, unpublished data). The EP2-R may serve as a second guard in case EP4-R-expression is affected by means of various combinations of inflammatory stimuli. In this respect, for the better understanding of contribution of EP2-R and EP4-R in physiological conditions, expressional changes in these receptors should be explored in various settings.

Acknowledgements

This work was supported by the Deutsche Forschungsgemeinschaft through the Sonderforschungsbereich 402, Teilprojekt B6, the Graduiertenkolleg 335, Fonds der Chemischen Industrie, the Japan Society for the Advancement of Science (fellowship to G.P.P.) and the German Association for the Study of the Liver (fellowship to A.F.).

References

[1] Kuiper J, Zijlstra FJ, Kamps JA, van Berkel TJ. Identification of prostaglandin D_2 as the major eicosanoid from liver endothelial and Kupffer cells. Biochim Biophys Acta 1988;959:143–152.
[2] Dieter P, Peters T, Schulze-Specking A, Decker K. Independent regulation of thromboxane and prostaglandin synthesis in liver macrophages. Biochem Pharmacol 1989;38:1577–1581.

[3] Hespeling U, Püschel GP, Jungermann K, Götze O, Zwirner J. Stimulation of glycogen phosphorylase in rat hepatocytes via prostanoid release from Kupffer cells by recombinant rat anaphylatoxin C5a but not by native human C5a in hepatocyte/Kupffer cell co-cultures. FEBS Lett 1995;372:108–112.
[4] Püschel GP, Hespeling U, Oppermann M, Dieter P. Increase in prostanoid formation in rat liver macrophages (Kupffer cells) by human anaphylatoxin C3a. Hepatology 1993;18:1516–1521.
[5] Peters T, Gaillard T, Decker K. Tumor necrosis factor alpha stimulates prostaglandin but not superoxide synthesis in rat Kupffer cells. Eicosanoids 1990;3:115–120.
[6] Casteleijn E, Kuiper J, Van Rooij HC, Kamps JA, Koster JF, Van Berkel TJ. Endotoxin stimulates glycogenolysis in the liver by means of intercellular communication. J Biol Chem 1988;263:6953–6955.
[7] Püschel GP, Kirchner C, Schröder A, Jungermann K. Glycogenolytic and antiglycogenolytic prostaglandin E_2 actions in rat hepatocytes are mediated via different signalling pathways. Eur J Biochem 1993;218:1083–1089.
[8] Brass EP, Garrity MJ. Effect of E-series prostaglandins on cyclic AMP-dependent and -independent hormone-stimulated glycogenolysis in hepatocytes. Diabetes 1985;34:291–294.
[9] Bronstad GO, Christoffersen T. Inhibitory effect of prostaglandins on the stimulation by glucagon and adrenaline of formation of cyclic AMP in rat hepatocytes. Eur J Biochem 1981;117:369–374.
[10] Püschel GP, Christ B. Inhibition by PGE_2 of glucagon-induced increase in phosphoenolpyruvate carboxykinase mRNA and acceleration of mRNA degradation in cultured rat hepatocytes. FEBS Lett 1994;351:353–356.
[11] Schieferdecker HL, Pestel S, Püschel GP, Götze O, Jungermann K. Increase by anaphylatoxin C5a of glucose output in perfused rat liver via prostanoids derived from non-parenchymal cells: direct action of prostaglandins and indirect action of thromboxane A(2) on hepatocytes. Hepatology 1999;30:454–461.
[12] Fennekohl A, Lucas M, Püschel GP. Induction by interleukin-6 of Gs-coupled prostaglandin E_2 receptors in rat hepatocytes mediating a prostaglandin E_2-dependent inhibition of the hepatocyte's acute phase response. Hepatology 2000;31:1128–1134.
[13] Kawada N, Tran-Thi TA, Klein H, Decker K. The contraction of hepatic stellate (Ito) cells stimulated with vasoactive substances. Possible involvement of endothelin 1 and nitric oxide in the regulation of the sinusoidal tonus. Eur J Biochem 1993;213:815–823.
[14] Kawada N, Klein H, Decker K. Eicosanoid-mediated contractility of hepatic stellate cells. Biochem J 1992;285:367–371.
[15] Wang XE, Watanabe S, Oide H, Hirose M, Itatsu T, Osada T, et al. Hepatic stellate cell contraction is inhibited by lipo-prostaglandin E1 in vitro. J Gastroenterol Hepatol 1998;13:S14–S18.
[16] Harbrecht BG, Kim YM, Wirant EA, Simmons RL, Billiar TR. Timing of prostaglandin exposure is critical for the inhibition of LPS- or IFN-gamma-induced macrophage NO synthesis by PGE_2. J Leukoc Biol 1997;61:712–720.
[17] Harbrecht BG, McClure EA, Simmons RL, Billiar TR. Prostanoids inhibit Kupffer cell nitric oxide synthesis. J Surg Res 1995;58:625–629.
[18] Goss JA, Mangino MJ, Callery MP, Flye MW. Prostaglandin E_2 downregulates Kupffer cell production of IL-1 and IL-6 during hepatic regeneration. Am J Physiol 1993;264:G601–G608.
[19] Peters T, Karck U, Decker K. Interdependence of tumor necrosis factor, prostaglandin E_2, and protein synthesis in lipopolysaccharide-exposed rat Kupffer cells. Eur J Biochem 1990;191:583–589.
[20] Reinstein LJ, Lichtman SN, Currin RT, Wang J, Thurman RG, Lemasters JJ. Suppression of lipopolysaccharide-stimulated release of tumor necrosis factor by adenosine: evidence for A_2 receptors on rat Kupffer cells. Hepatology 1994;19:1445–1452.
[21] Coleman RA, Eglen RM, Jones RL, Narumiya S, Shimizu T, Smith WL, et al. Prostanoid and leukotriene receptors: a progress report from the IUPHAR working parties on classification and nomenclature. Adv Prostaglandin Thromboxane Leukot Res 1995;23:283–285.
[22] Negishi M, Sugimoto Y, Ichikawa A. Prostaglandin E receptors. J Lipid Mediat Cell Signal 1995;12:379–391.
[23] Fennekohl A, Schieferdecker HL, Jungermann K, Püschel GP. Differential expression of prostanoid receptors in hepatocytes, Kupffer cells, sinusoidal endothelial cells and stellate cells of rat liver. J Hepatol 1999;30:38–47.
[24] Hizaki H, Segi E, Sugimoto Y, Hirose M, Saji T, Ushikubi F, et al. Abortive expansion of the cumulus and impaired fertility in mice lacking the prostaglandin E receptor subtype EP2. Proc Natl Acad Sci USA 1999;96:10501–10506.
[25] Segi E, Sugimoto Y, Yamasaki A, Aze Y, Oida H, Nishimura T, et al. Patent ductus arteriosus and neonatal death in prostaglandin receptor EP4-deficient mice. Biochem Biophys Res Commun 1998;246:7–12.
[26] Nguyen M, Camenisch T, Snouwaert JN, Hicks E, Coffman TM, Anderson PA, Malouf NN, et al. The prostaglandin receptor EP4 triggers remodelling of the cardiovascular system at birth. Nature 1997;390:78–81.
[27] Katsuyama M, Ikegami R, Karahashi H, Amano F, Sugimoto Y, Ichikawa A. Characterization of the LPS-stimulated expression of EP2 and EP4 prostaglandin E receptors in mouse macrophage-like cell line, J774.1. Biochem Biophys Res Commun 1998;251:727–731.
[28] Nishigaki N, Negishi M, Ichikawa A. Two Gs-coupled prostaglandin E receptor subtypes, EP2 and EP4, differ in desensitization and sensitivity to the metabolic inactivation of the agonist. Mol Pharmacol 1996;50:1031–1037.
[29] Blaschke V, Jungermann K, Püschel GP. Exclusive expression of the Gs-linked prostaglandin E_2 receptor subtype 4 mRNA in mononuclear Jurkat and KM-3 cells and coexpression of subtype 4 and 2 mRNA in U-937 cells. FEBS Lett 1996;394:39–43.
[30] Noguchi K, Iwasaki K, Shitashige M, Ishikawa I. Prostaglandin E_2 receptors of the EP2 and EP4 subtypes downregulate tumor necrosis factor alpha-induced intercellular adhesion molecule-1 expression in human gingival fibroblasts. J Periodontal Res 1999;34:478–485.
[31] Kiriyama M, Ushikubi F, Kobayashi T, Hirata M, Sugimoto Y, Narumiya S. Ligand binding specificities of the eight types and subtypes of the mouse prostanoid receptors expressed in Chinese hamster ovary cells. Br J Pharmacol 1997;122:217–224.
[32] Dieter P, Hempel U, Kamionka S, Kolada A, Malessa B, Fitzke E, et al. Prostaglandin E_2 affects differently the release of inflammatory mediators from resident macrophages by LPS and muramyl tripeptides. Mediators Inflamm. 1999;8:295–303.
[33] Grewe M, Gausling R, Gyufko K, Hoffmann R, Decker K. Regulation of the mRNA expression for tumor necrosis factor-alpha in rat liver macrophages. J Hepatol. 1994;20:811–818.
[34] Shames BD, McIntyre Jr RC, Bensard DD, Pulido EJ, Selzman CH, Reznikov LL, et al. Suppression of tumor necrosis factor alpha production by cAMP in human monocytes: dissociation with mRNA level and independent of interleukin-10. J Surg Res. 2001;99:187–193.
[35] Choi SS, Gatanaga M, Granger GA, Gatanaga T. Prostaglandin-E_2 regulation of tumor necrosis factor receptor release in human monocytic THP-1 cells. Cell Immunol. 1996;170:178–184.

Biochemical and Biophysical Research Communications 290, 696–700 (2002)
doi:10.1006/bbrc.2001.6256, available online at http://www.idealibrary.com on IDEAL®

Expression of Prostaglandin E_2 Receptor Subtypes in Mouse Hair Follicles

Eiko Torii,* Eri Segi,* Yukihiko Sugimoto,* Kenzo Takahashi,† Kenji Kabashima,† Kohichi Ikai,† and Atsushi Ichikawa*,[1]

Department of Physiological Chemistry, Faculty of Pharmaceutical Sciences, Kyoto University, Sakyo-ku, Kyoto 606-8501, Japan; and †Department of Dermatology, Kyoto University, Graduate School of Medicine, Sakyo-ku, Kyoto 606-8507, Japan

Received December 7, 2001

We investigated the mRNA distribution of the prostaglandin (PG) E_2 receptor subtypes and cyclooxygenases (COXs) in hair follicles of the mouse dorsal skin. In the 3-week hair follicles, which are in the anagen phase, EP3 and EP4 mRNA were expressed in the dermal papilla cells and the outer root sheath cells located in the hair bulb region, respectively. In the 8-week hair follicles, which are in the telogen phase, the signals for both EP3 and EP4 mRNAs had disappeared. To study the hair cycle-dependent expression of mRNAs for the EPs and COXs, an area of dorsal hair was depilated from 8-week-old mice. On days 8 and 12 after depilation, EP3 and EP4 mRNA were reexpressed in the dermal papilla cells and the outer root sheath cells, and the induction of COX-2 mRNA was also observed in the outer root sheath cells, the upper area of EP4 expression site. These results suggest that EP3 and EP4 receptors may involve in the development and regrowth of the hair follicles. © 2002 Elsevier Science

Key Words: **prostaglandin; receptor; cyclooxygenase; hair follicle; skin; *in situ* hybridization; dermal papilla; outer root sheath.**

Hair growth is the cumulative result of a series of processes involving cellular proliferation and differentiation within a hair follicle (1). Hair follicles are epidermal-derived appendages that arise as a result of the inducible effects of specialized dermal fibroblasts acting on stem cells. The stem cells in the bulge area of a hair follicle migrate out and then enter a period of differentiation and massive proliferation that culminates in the formation of a mature hair follicle. In mammals, the hair growth cycle is known to consist of three phases: (i) anagen, when the follicles grow, hair synthesis takes place and the skin becomes thick; (ii) catagen, when the follicles regress and the skin becomes thin; and (iii) telogen, when the follicles and skin are at rest (2, 3). Evidence indicates that the process of hair growth is regulated by a variety of physiological factors such as hormones, growth factors, cytokines and adhesion molecules (4–6).

In addition, prostaglandin E_2 (PGE_2), one of the cyclooxygenase (COX)-metabolites of arachidonic acid, has been known to be involved in hair growth. For example, it has been reported that aspirin-like drugs, which are COX inhibitors, induce hair loss in humans (7, 8), and that the topical or systematic administration of a PGE_2 analog protected mice from radiation-induced alopecia (9). These findings show that PGE_2 may have a role in the stimulation of hair growth. Furthermore, one of the therapeutic effects of minoxidil, a hair growth stimulator, is assumed to be due to its stimulation of PGE_2 synthesis, which results in the induction and prolongation of the anagen stage of normal hair growth (10).

COX activity has been demonstrated to be present in rodent skin (11, 12), most probably in the fibroblasts and keratinocytes (13–15), and the major arachidonic acid metabolite in the skin was found to be PGE_2. Two COX isoforms have been identified, which exhibit similar catalytic activities but distinctive patterns of expression (16). Müller-Decker *et al.* have been reported that the COX-1 protein is present in keratinocytes which locate in the interfollicular epidermis and the upper part of the hair follicle, and that COX-2 protein is induced in the basal layer of the interfollicular epidermis in mouse skin treated with 12-*O*-tetradecanoylphorbol 13-acetate (17).

The PGE receptors are genetically subdivided into four subtypes having different structures and signal transduction pathways; EP1 is coupled to the stimulation of intracellular Ca^{2+} mobilization, EP2 and EP4 are coupled to the stimulation of adenylate cyclase, and EP3 is coupled to the inhibition of adenylate cyclase (18, 19). PGE_2 is known to be involved in a variety of physiological functions and has been found to play a

[1] To whom correspondence and reprint requests should be addressed. Fax: +81-75-753-4557. E-mail: aichikaw@pharm.kyoto-u.ac.jp.

0006-291X/02 $35.00

role in skin regeneration and hair growth (15). However, it has not been defined as to which of the specific PGE receptor subtypes mediate each of the many steps of hair growth process.

Here we examined the tissue distribution of the transcripts for the EP receptor subtypes and COX isozymes in the hair follicles of the 3-week-old back skin, and to clarify these expression pattern in the hair regrowth cycle, we examined the expression pattern of EPs and COXs mRNA in the hair follicles during the depilation-induced hair regrowth.

MATERIALS AND METHODS

Animals. For the study of mRNA expression in normal skin, male C57BL/6 mice were used (3 and 8 weeks of age) (SLC Inc., Hamamatsu, Japan). All experiments were conducted in accordance with the ethical standards established by the institutional animal care and use committee of the Kyoto University. Animals were maintained at 23°C under a 12-h light cycle, fed a normal diet and provided with water *ad libitum*.

Hair cycle induction. Male C57BL/6 mice at 8 weeks of age in the telogen stage of the hair cycle were used. The mice were anesthetized with sodium pentobarbital injected intraperitoneally. An area (2.5 cm × 3.0 cm) on the back of the mice was depilated with a commercial depilatory agent as previously described (20). Anagen starts synchronously in all hair follicles at the time of depilation. Mice were analyzed at specific time points after depilation.

In situ hybridization. In situ hybridization was carried out as described previously (21). For the study of depilation-induced hair follicles, the skin on the backs of mice were dissected 3, 5, 8, 12, 18, and 26 days after depilation, and just before depilation, and immediately frozen. Sections 10 μm thick were cut on a Jung Frigocut 3000E cryostat and thaw-mounted onto poly-L-lysine-coated glass slides. Antisense riboprobes were synthesized by transcription with T3 or T7 RNA polymerase (Stratagene, La Jolla, CA) in the presence of [α-^{35}S]CTP for *in situ* hybridization. The sections were fixed with 4% formalin and acetylated with 0.25% acetic anhydride. Hybridization was carried out in a buffer containing 50% formamide, 2 × SSC (1 × SSC is composed of 0.15 M NaCl and 0.015 M sodium citrate), 10 mM tris(hydroxymethyl)aminomethane-Cl, pH 7.5, 1 × Denhardt's solution, 10% dextran sulfate, 0.2% sodium dodecyl sulfate (SDS), 100 mM dithiothreitol, 500 μg/ml sheared single-stranded salmon sperm DNA, and 250 μg/ml yeast tRNA. The riboprobes were added to the hybridization buffer at 1.5 × 10^5 cpm/μl. After incubation at 60°C for 5 h, the slides were washed for 1 h in 2× SSC. The sections were treated with 20 μg/ml ribonuclease A, followed by an additional wash in 0.1× SSC at 60°C for 1 h. The slides were then dipped in nuclear track emulsion (NTB3, Eastman Kodak, Rochester, NY). After exposure for 5 weeks at 4°C, the dipped slides were developed, fixed, and counterstained with hematoxylin and eosin. The specificity of the signals for each probe was determined by hybridizing with the sense probe and adding an excess amount of the unlabeled antisense probe, both of which did not produce specific signals. These experiments were repeated three times with different animals, and identical results were obtained.

RESULTS

Expression of mRNA for the PGE Receptor Subtypes and COXs in the Hair Follicle of 3-Week-Old Mouse Back Skin

We first examined the expression patterns of mRNAs for the various PGE receptor subtypes and COXs in the hair follicle of 3-week-old mouse skin by *in situ* hybridization. In this period most of hair follicles are in the late of first anagen phase (Fig. 1A) and intensive mRNA signals for EP3 and EP4 were observed. The black grain signals for EP3 mRNA was localized in the dermal papilla cells (Fig. 1B). The brown dots above the black grains show the growing hair shaft. EP4 mRNA was abundantly expressed in the outer root sheath cells, but the signals were restricted to the hair bulb region, the lower most portion of the hair follicle (Fig. 1D). While we detected the COX-1 mRNA signals in the epidermal cells and the EP3 mRNA signals in the fibroblast cells, no signals for the mRNA of EP1, EP2 and COX-2 could be detected in the hair follicles of 3-week old mouse skin (data not shown). Hybridization signals for sense probes were not detected (Fig. 1C in EP3 sense probe and data not shown).

Expression of EP3, EP4 and COX-2 mRNA in the Hair Follicles of the Hair Regrowth Induced Back Skin

We next examined the mRNA expression of both EP3 and EP4 in the hair follicle of 8-week old mouse back skin. Morphologically, hair follicles were sparse and most were regressed, suggesting that they were in the telogen phase (Fig. 2A). The mRNA expression of both EP3 and EP4 could no longer be observed in the hair follicles of the telogen phase (Figs. 2B and 2C). To clarify the expression of EP3 and EP4 subtypes in relation to the hair regrowth cycle, an area of dorsal hair was depilated with a commercial depilatory agent in 8-week-old mice and the EP3 and EP4 mRNA expression was analyzed by *in situ* hybridization analysis during hair regrowth process. The development of hair follicles are apparent and new hairs begin to grow on day 8 after depilation (Fig. 2D), and hair follicles are fully growing by day 12 after depilation (Fig. 2G). On days 8 and 12, the hair follicles in depilated skin express both EP3 mRNA in dermal papilla cells (Figs. 2E and 2H) and EP4 mRNA in the outer root sheath cells, respectively (Fig. 2F and 2I), as seen in the 3-week-old mouse hair follicles. These results suggest that EP3 and EP4 receptor play a role in the development and regrowth of the hair follicles. Interestingly, we found COX-2 mRNA induction in the outer root sheath cells of the hair follicles on days 8 and 12 after depilation (Figs. 3A and 3B), which were not observed in 3-week old hair follicles. This COX-2 mRNA signals were found in the upper area of the hair bulb, whereas EP4 mRNA signals in the outer root sheath were localized in the lower area of the hair bulb.

DISCUSSION

We have shown here that two subtypes of the PGE receptor, EP3 and EP4, are expressed in different com-

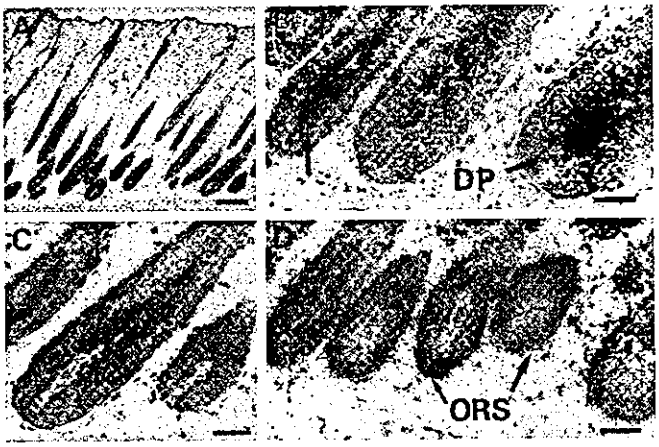

FIG. 1. The EP3 and EP4 transcripts are expressed in the hair follicles of the skin of 3-week-old mice. (A) The section of the 3-week-old back skin stained with hematoxylin and eosin is shown. (B, C, D) Brightfield photomicrographs of the skin sections hybridized with ^{35}S-labeled antisense riboprobe for the EP3 (B) and EP4 (D) mRNA and sense riboprobe for the EP3 (C) mRNA. Autoradiographic grains for EP3 mRNA and EP4 mRNA are confined to the dermal papilla cells (arrows in B) and outer root sheath cells (arrows in D), respectively. DP, dermal papilla cells; ORS, outer root sheath cells. Bars, 200 μm (A), and 50 μm (B, C, D).

ponents of the anagen hair follicles. This is the first report showing the involvement of PGE receptor subtypes in the hair follicle development and regrowth. In addition, we found that transient COX-2 mRNA expression is induced during the depilation-induced anagen phase, and this expression is concentrated in the upper area of the hair bulb, suggesting the prostanoid biosynthesis pathway via COX-2 at this hair bulb region during early anagen phase.

A high level of EP3 mRNA expression was found in the dermal papilla cells during the anagen phase. The dermal papilla cells are originated from fibroblast cells and induce hair follicle formation from the overlying epithelium during development, and interact with secondary germ cells to regenerate the lower follicle at the onset of a new follicle cycle in adults (1). Since PGE_2 is known to play roles in the proliferation and differentiation of fibroblasts and in the induction of vascular endothelial growth factor (14, 22, 23), the EP3 receptor may be involved in functions of the dermal papilla such as angiogenesis and differentiation during the anagen phase. On the other hand, EP4 mRNA was expressed

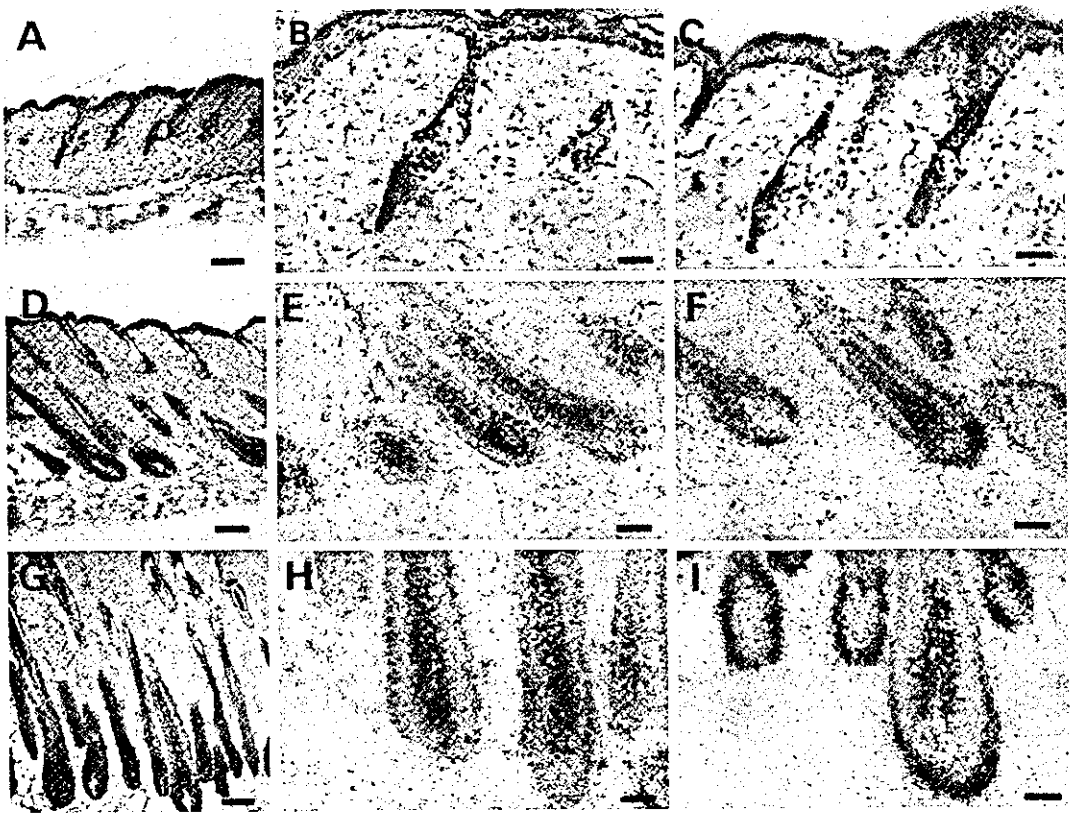

FIG. 2. EP3 and EP4 transcripts are detected in the hair follicles of depilation-treated 8-week mouse skin. (A, D, G) An area on the 8-week-old back skin was depilated with a commercial depilatory agent and the development of depilation-induced anagen hair follicles was examined morphologically. The sections before treatment (A), 8 days (D), and 12 days (G) after treatment stained with hematoxylin and eosin are shown. (B, E, H) Brightfield photomicrographs of the skin sections hybridized with ^{35}S-labeled antisense riboprobe for the EP3 mRNA before treatment (B), 8 days (E), and 12 days (H) after treatment. Autoradiographic grains for EP3 mRNA are confined to the dermal papilla cells. (C, F, I) Brightfield photomicrographs of the skin sections hybridized with ^{35}S-labeled antisense riboprobe for the EP4 mRNA before treatment (C), 8 days (F), and 12 days (I) after treatment. Autoradiographic grains for EP4 mRNA are confined to the outer root sheath cells. Bars, 150 μm (A, D, G), and 50 μm (B, C, E, F, H, I).

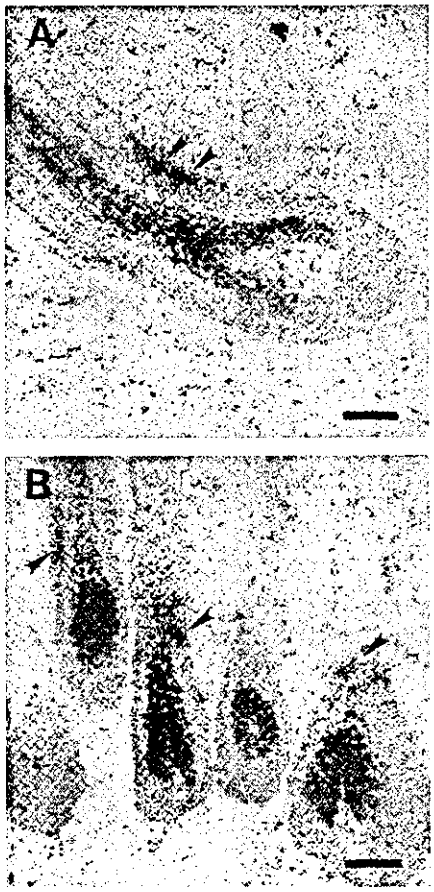

FIG. 3. COX-2 transcripts are detected in the hair follicles of depilation-treated skin. (A, B) Brightfield photomicrographs of the skin sections hybridized with ^{35}S-labeled antisense riboprobe for the COX-2 mRNA 8 days (A) and 12 days (B) after depilation treatment. Autoradiographic grains for COX-2 mRNA are confined to the outer root sheath cells. Note that hybridization signals for COX-2 mRNA are confined to a few layers of outer root sheath cells, neighboring the cells expressing EP4 mRNA. Arrowheads show cells labeled with COX-2 mRNA probe. Bars, 150 μm.

in the outer root sheath of the bulb area, which is an area of terminal dilation of the hair follicle and where hair compartments differentiate and proliferate. Although the precise roles of the outer root sheath cells in the hair follicles are not well elucidated, recent studies have suggested that this component is important not only to protect the structure of the hair follicles but also to differentiate the various hair follicle components such as inner root sheath and hair shaft from the multipotent stem cells (24). The EP4 receptor subtype is coupled to the Gs protein, resulting in the activation of adenylate cyclase. Although the effect of cAMP on hair growth is not clear, Dubrasky *et al.* reported that an intraperitoneal injection of dibutyryl cAMP before radiation resulted in a higher survival of hair follicles (25). It will be important to investigate the effect of cAMP and an EP4 agonist on hair follicle growth.

We have also found the COX-2 mRNA expression in the depilation-induced hair follicles on day 8 and 12 after depilation. It is interesting that this COX-2 induction was not detected in the 3-week hair follicles, which is at the first (morphological) anagen phase. This result may indicate that PGE_2 have a role for hair regrowth in the some inflammatory situation rather than during the normal hair follicle development. Both the expression of EP4 and COX-2 mRNA was observed around the hair bulb area, but the expression patterns of both EP4 and COX-2 transcripts were strictly regulated; EP4 mRNA was expressed in the outer root sheath of the bulb area and the site of COX-2 mRNA expression was just above the area expressing EP4 mRNA. Both EP4 and COX-2 expression patterns seem to be unique compared with that of various molecules involved in the hair growth, such as cytokines and adhesion molecules (26). It is interesting to elucidate what molecules stimulate expression patterns of EP4 and COX-2 observed in specific areas of the hair follicles. Many reports have been suggested the role of PGE_2 as a stimulator for the hair growth (7–9). However, Neufang *et al.* recently reported that the transgenic mouse lines, which constitutively express COX-2 in the basal cells of the interfollicular epidermis and the pilosebaceous unit, exhibited delayed hair follicle morphogenesis, reduced hair follicle density, sebaceous gland hyperplasia and profound hyperplasia in scale epidermis of the tail (27). These results seem to imply the inhibitory role of COX-2 at least for hair follicle morphogenesis. A possible role of prostanoids in the process of hair follicle morphogenesis should be explored.

The present study indicates that expression of the EP receptor subtypes in hair follicles of mice occur in two distinct parts; EP4 mRNA is expressed in the outer root sheath of the bulb area, and EP3 mRNA is expressed in dermal papilla cells during the anagen phase. Interestingly, transient COX-2 mRNA expression is induced during the depilation-induced anagen phase, and this expression is concentrated in the upper area of the hair bulb. In humans, COX-1 is mainly expressed in the dermal papilla cells and it has been proposed that the mechanism of action of hair growth stimulation by minoxidil is via the activation of COX-1 (10). In our study, signals for neither COX-1 nor COX-2 mRNA could be detected in the dermal papilla of mouse hair follicles. It should therefore be examined whether PGE receptor expression patterns differ between species. These results suggest that COX-2, EP3 and EP4 receptors may involve in the development and regrowth of the mouse hair follicles.

ACKNOWLEDGMENTS

We thank K. Tsuboi for valuable advice and generous support. We are grateful to H. A. Popiel for careful reading of the manuscript and